

A GEOMETRIC LITTLEWOOD-RICHARDSON RULE

RAVI VAKIL

ABSTRACT. We describe an explicit geometric Littlewood-Richardson rule, interpreted as deforming the intersection of two Schubert varieties so that they break into Schubert varieties. There are no restrictions on the base field, and all multiplicities arising are 1; this is important for applications. This rule should be seen as a generalization of Pieri's rule to arbitrary Schubert classes, by way of explicit homotopies. It has a straightforward bijection to other Littlewood-Richardson rules, such as tableaux and Knutson and Tao's puzzles.

This gives the first geometric proof and interpretation of the Littlewood-Richardson rule. It has a host of geometric consequences, described in [V2]. The rule also has an interpretation in K -theory, suggested by Buch, which gives an extension of puzzles to K -theory. The rule suggests a natural approach to the open question of finding a Littlewood-Richardson rule for the flag variety, leading to a conjecture, shown to be true up to dimension 5. Finally, the rule suggests approaches to similar open problems, such as Littlewood-Richardson rules for the symplectic Grassmannian and two-flag varieties.

CONTENTS

1. Introduction	1
2. The Geometric Littlewood-Richardson rule: Combinatorial description	4
3. Describing the geometry of the Grassmannian and flag variety with checkers	11
4. Application: Littlewood-Richardson rules	16
5. Bott-Samelson Varieties	22
6. Proof of the Geometric Littlewood-Richardson rule	27
7. Appendix: The bijection between checker games and puzzles (with A. Knutson)	41
References	44

1. INTRODUCTION

The goal of this note is to describe an explicit geometric Littlewood-Richardson rule, interpreted as deforming the intersection of two Schubert varieties (with respect to transverse flags F and M .) so that they break into Schubert varieties. There are no restrictions on the base field, and all multiplicities arising are 1; this is important for applications. This rule should be seen as a generalization of Pieri's rule to arbitrary Schubert classes, by way

Date: Saturday, February 22, 2003.

1991 *Mathematics Subject Classification.* Primary 14M15, 14N15; Secondary 05E10, 05E05.

Partially supported by NSF Grant DMS-0228011, an AMS Centennial Fellowship, and an Alfred P. Sloan Research Fellowship.

of explicit homotopies. It has a straightforward bijection to other Littlewood-Richardson rules, such as tableaux (Sect. 2.6) and Knutson and Tao's puzzles [KTW, KT] (Sect. 7).

This gives the first geometric proof and interpretation of the Littlewood-Richardson rule. It has a host of geometric consequences, described in [V2]. The rule also has an interpretation in K -theory, suggested by Buch (Sect. 4.3), which suggests an extension of puzzles to K -theory (Theorem 4.6), yielding a triality of K -theory Littlewood-Richardson coefficients. The rule suggests a natural approach to the open question of finding a Littlewood-Richardson rule for the flag variety, leading to a conjecture, shown to be true up to dimension 5 (Sect. 4.8). Finally, the rule suggests approaches to similar open problems, such as Littlewood-Richardson rules for the symplectic Grassmannian and two-flag varieties, and the quantum cohomology of the Grassmannian (Sect. 4.11).

The strategy is as follows. We degenerate the "Moving flag" M through a series of codimension one degenerations (in $Fl(n)$) in a particular way (the "specialization order") so that the cycle in $G(k, n)$ successively breaks into varieties we can easily understand ("two-flag Schubert varieties"). At each stage, the cycle breaks into one or two pieces, and each piece appears with multiplicity one (a key fact for applications). At the end M coincides with the "Fixed flag" F , and the limit cycle is a union of Schubert varieties with respect to this flag. An explicit example is shown in Figure 6. (*Caution:* the theorem is stated in terms of the affine description of the Grassmannian, but all geometric descriptions are in terms of projective geometry. Hence Figure 6 shows a calculation in $G(2, 4)$ using lines in \mathbb{P}^3 .)

We note that degeneration methods are a very old technique. See [K12] for a historical discussion. Sottile suggests that [P] is an early example, proving Pieri's formula using such methods; see also Hodge's proof [H]. More recent work by Sottile (especially [S1], dealing with $G(2, n)$, and [S2], concerning Pieri's formula in general) provided inspiration for this work.

The degenerations can be described combinatorially, in terms of black and white checkers on an $n \times n$ checkerboard. Thus Littlewood-Richardson coefficients count "checker games". The input is the data of two Schubert varieties, in the form of two k -subsets of $\{1, \dots, n\}$; each move corresponds to moving black checkers (encoding the position of M) in a certain way (the "specialization order"), and determining then how the white checkers (encoding the position of the k -plane) move. The output is interpreted as set of k -subsets. Similarly, Schubert problems (i.e. intersecting many Schubert classes) count "checker tournaments". The checker rule is easy to use in practice, but somewhat awkward to describe. However, at all steps, (i) its geometric meaning is clear at all steps, and (ii) there is a straightforward bijection to partially completed tableaux and puzzles. For many geometric applications [V2], the details of the combinatorial rule are unnecessary. R. Moriarty has written a program implementing this rule.

1.1. Remarks on positive characteristic. We note that the only two characteristic-dependent statements in the paper are invocations of the Kleiman-Bertini theorem [K11] (Sections 3.7 and 3.11). Neither is used for the proof of the main theorem (Theorem 3.10).

They will be replaced by a characteristic-free generic smoothness theorem [V2, Thm. 2.6] proved *using* the Geometric Littlewood-Richardson rule.

1.2. Overview of paper. Section 2 is a description of the rule in combinatorial terms; it contains no geometry.

Section 3 describes the geometry related to “two-flag Schubert varieties” in the Grassmannian in the language of checkers. Black checkers correspond to the relative position of the two flags; white checkers correspond to the k -plane. The main theorem (Theorem 3.10) is stated here. Geometrically-minded readers may prefer to read some of Section 3 before Section 2.

The proof makes repeated use of smooth “Bott-Samelson varieties” $BS(\mathcal{P})$ corresponding to a “planar poset” \mathcal{P} . They are simple objects, and some basic properties are described in Section 5. Of particular importance is the Bott-Samelson variety $BS(\mathcal{P}_\square)$ parametrizing two hyperplanes and a codimension two plane contained in both. Each step in the degeneration is related to $BS(\mathcal{P}_\square)$ via the key construction of Section 5.6.

The proof of the Geometric Littlewood-Richardson rule is given in Section 6; the strategy is outlined in Section 6.1.

Applications are discussed in Section 4. Some are proved in detail, while others are merely sketched. Further geometric applications are discussed in [V2].

1.3. Summary of notation. If $X \subset Y$, let $\text{Cl}_Y X$ denote the closure in Y of X . Fix a base field K (of any characteristic, not necessarily algebraically closed), and non-negative integers $k \leq n$. We work in $G(k, n)$, the Grassmannian of dimension k subspaces of K^n .

We follow the notation of [F]. For example, let Ω_w denote the Schubert class in $H^*(G(k, n))$ or $A^*(G(k, n))$ (resp. $H^*(Fl(n))$ or $A^*(Fl(k, n))$), where w is a partition (resp. a permutation). Let $\Omega_w(F)$ (resp. $\Omega_w^\circ(F)$) be the closed (resp. open) Schubert variety with respect to the flag F . In $Fl(n)$,

$$\Omega_w(F) = \{[V] \in Fl(n) : \dim(V_p \cap F_q) \geq \#\{i \leq p : w(i) > n - q\} \text{ for all } p, q\}.$$

The Schur polynomials are denoted s .

Table 1 is a summary of notation introduced in the article.

1.4. Acknowledgments. The author is grateful to A. Buch and A. Knutson for patiently explaining the combinatorial, geometric, and representation-theoretic ideas behind this problem, and for comments on earlier versions. Any remaining misunderstandings are purely due to the author. The author also thanks L. Chen, W. Fulton, R. Moriarty, and F. Sottile.

section introduced	notation
2.1–2.3	configuration of checkers, specialization order, descending and rising checkers, \bullet , \bullet_{init} , \bullet_{final} , \bullet_{next} , happy, \circ , $\circ\bullet$, $\circ_{A,B}$, critical row, critical diagonal, Phase 1, swap, blocker, Phase 2, \circ_{stay} , \circ_{swap} , \circ_S
2.8	mid-sort
3.1	M , F , dominate, X .
3.4	open and closed two-flag Schubert varieties $Y_{\bullet\bullet}$ and $\bar{Y}_{\bullet\bullet}$, universal two-flag Schubert variety, $X_{\bullet\bullet}$, $\bar{X}_{\bullet\bullet}$.
3.8	D_X
5.1	dimension, planar poset, \mathcal{P} , quadrilateral, southwest and northeast border, Bott-Samelson variety, $BS(\mathcal{P})$
5.3–5.5	strata of a Bott-Samelson variety, \mathcal{P}_{\bullet} , \mathcal{P}_{\circ} , $BS(\mathcal{P} \rightarrow \mathcal{Q})$, $p_{\circ\bullet}$.
5.6–5.8	\mathcal{P}_{\square} , x , y , y' , z , V_x , V_y , $V_{y'}$, V_z , D_{\square} , $p_{\bullet\square}$, (r, c) , S , T , $X_{\bullet\square}$, $X_{\bullet\square}$ -position
6.1	geometrically (ir)relevant
6.3	Z
6.6–6.8	a, a', a'' , left and right good quadrilaterals, columns, D_S^Z , D_S , Q_{ℓ} , \mathcal{P}'_{\circ} .

TABLE 1. Summary of notation

2. THE GEOMETRIC LITTLEWOOD-RICHARDSON RULE: COMBINATORIAL DESCRIPTION

2.1. Littlewood-Richardson coefficients $c_{\alpha\beta}^{\gamma}$ will be counted in their guise of structure constants of the cohomology (or Chow) ring of the Grassmannian $G(k, n)$, which in turn will be interpreted in terms of *checker games*, involving n black and k white checkers on an $n \times n$ board. The rows and columns of the board are numbered as in Figure 1; (r, c) will denote the square in row r and column c . A set of checkers on the board will be called a *configuration* of checkers.

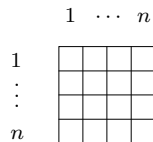


FIGURE 1.

2.2. Black checkers. The moves of the black checkers are prescribed in advance; the Littlewood-Richardson coefficients are counted by the possible accompanying moves of the white checkers.

No two checkers of the same color are in the same row or column. Hence the positions of the black checkers correspond to permutations by the following bijection: if the black checker in column c is in row r , then the permutation sends $n + 1 - c$ to r . For example, see Figure 2.

The initial position of the black checkers corresponds to the identity permutation in S_n , and the final position corresponds to the longest word w_0 . The intermediate positions in the checker game correspond to partial factorizations from the right of w_0 :

$$w_0 = e_{n-1} \cdots e_2 e_1 \quad \cdots \quad e_{n-1} e_{n-2} e_{n-3} \quad e_{n-1} e_{n-2} \quad e_{n-1}.$$

For example, in Figure 2 shows the six moves of the black checkers for $n = 4$, along with the corresponding permutations. (The geometric interpretation will be explained in Sect. 3.3.) In essence this is a bubble-sort. Call this the *specialization order* in the Bruhat order. Figure 3 shows a typical checker configuration in the specialization order. Each move will involve moving one checker one row down (call this the *descending checker*), and another checker (call this the *rising checker*) one row up, as shown in the figure.

Note that this word neither begins nor ends with the corresponding word for $n - 1$, making induction impossible (see Sect. 3.12).

We will use the notation \bullet to represent a configuration of black checkers. Denote the initial configuration by \bullet_{init} , and the final configuration by \bullet_{final} . If \bullet is one of the configurations in the specialization order, and $\bullet \neq \bullet_{\text{final}}$, then \bullet_{next} will denote the next configuration in the specialization order.

2.3. White checkers. At each stage of the game, each white checker has the following property: there is a black checker in the same square or in a square above it, and there is a black checker in the same square or in a square to the left of it. A white checker satisfying this property is said to be *happy*. (In particular, a white checker is happy if it is in the same square as a black checker.) A configuration of white checkers will often be denoted \circ , and a configuration of white and black checkers will often be denoted $\circ\bullet$.

The initial position of the white checkers depends on two subsets $A = \{a_1, \dots, a_k\}$ and $B = \{b_1, \dots, b_k\}$ of $\{1, \dots, n\}$, where $a_1 < \dots < a_k$ and $b_1 < \dots < b_k$. The k white checkers are in the squares $(a_1, b_k), (a_2, b_{k-1}), \dots, (a_k, b_1)$. We denote this configuration by $\circ_{A,B}$. If (and only if) any of these white checkers are not happy (i.e. if $a_i + b_{k+1-i} \leq n$ for some i), then there are no checker games corresponding to (A, B) . (This will mean that all corresponding Littlewood-Richardson coefficients are 0. Geometrically, this means that the two Schubert varieties do not intersect.) This happens, for example, if $n = 2$ and $A = B = \{1\}$, computing the intersection of two general points in \mathbb{P}^1 .

For each move of the black checkers, there will be one or two possible moves of the white checkers, which we describe next. Define the *critical row* and the *critical diagonal* as in Figure 3. The movement of the white checkers takes place in two phases.

Phase 1 depends on the answers to the two questions: Where (if anywhere) is the white checker in the critical row? Where (if anywhere) is the highest white checker in the critical diagonal? (There may be several white checkers in the critical diagonal.)

Based on the answer to these questions, the pair of white checkers either swap rows (i.e. if the white checkers start at (r_1, c_1) and (r_2, c_2) , then they will end at (r_2, c_1) and (r_1, c_2)), or they stay where they are, according to Table 2. The central entry of the table is the only time when there is a possibility for choice: the pair of white checkers can stay, or *if there*

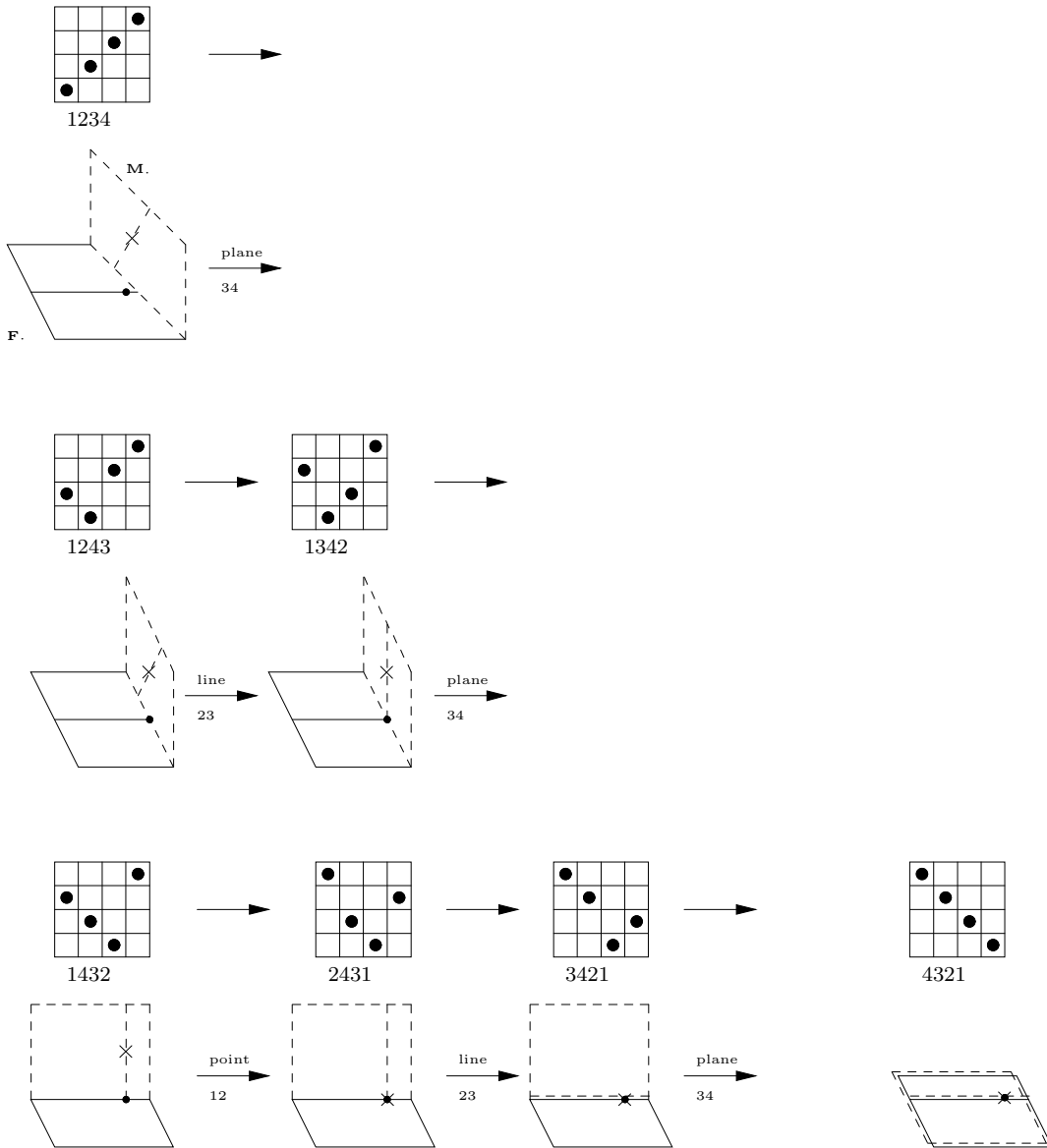


FIGURE 2. The *specialization order* for $n = 4$, in terms of checkers and permutations, with the geometric interpretation of Section 3

are no white checkers in the rectangle between them they can swap. Call white checkers in this rectangle *blockers*. See Figure 4 for an example of a blocker.

Phase 2 is a “clean-up phase”: if any white checkers are not happy, then move them by sliding them either left or up so that they become happy. This is always possible, in a unique way.

If $\circ\bullet$ corresponds to the configuration of black and white checkers before the move, we denote the one or two possible configurations after the move by $\circ_{\text{stay}}\bullet_{\text{next}}$ and/or $\circ_{\text{swap}}\bullet_{\text{next}}$. Examples of the ten cases are given in Figure 5.

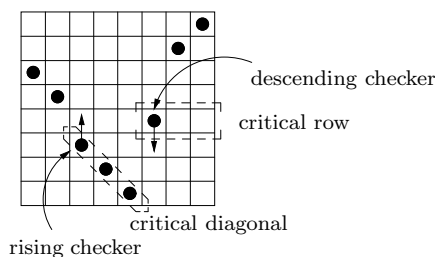


FIGURE 3. The critical row and the critical diagonal

		White checker in critical row?		
		yes, in descending checker's square	yes, elsewhere	no
Top white checker in critical diagonal?	yes, in rising checker's square	swap	swap	stay [†]
	yes, elsewhere	swap	swap if no blocker or stay	stay
	no	stay	stay	stay

TABLE 2. Phase 1 of the white checker moves (see Figure 5 for a pictorial description)

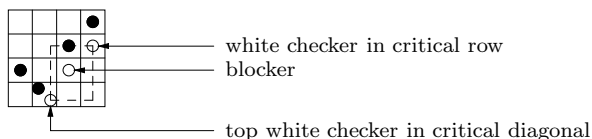


FIGURE 4. Example of a blocker

At the end of the checker game, the black checkers are in position \bullet_{final} , and as the white checkers are happy, they must lie on a subset of the black checkers. The corresponding output is again a subset S of $\{1, \dots, n\}$ of size k . Denote this final configuration of white checkers by \circ_S .

Hence to any two subsets A, B of $\{1, \dots, n\}$ of size k , we can associate a formal sum of subsets of size k , corresponding to checker games. Figure 6 illustrates the two checker games starting with $A = B = \{2, 4\}$ for $k = 2, n = 4$. The output consists of the two subsets $\{1, 4\}$ and $\{2, 3\}$. Figure 7 illustrates all checker games starting with $A = B = \{2, 4, 6\}$ for $k = 3, n = 6$. The output is $\{2, 3, 4\} + 2\{1, 3, 5\} + \{1, 2, 6\}$.

2.4. Littlewood-Richardson coefficients in terms of checker games.

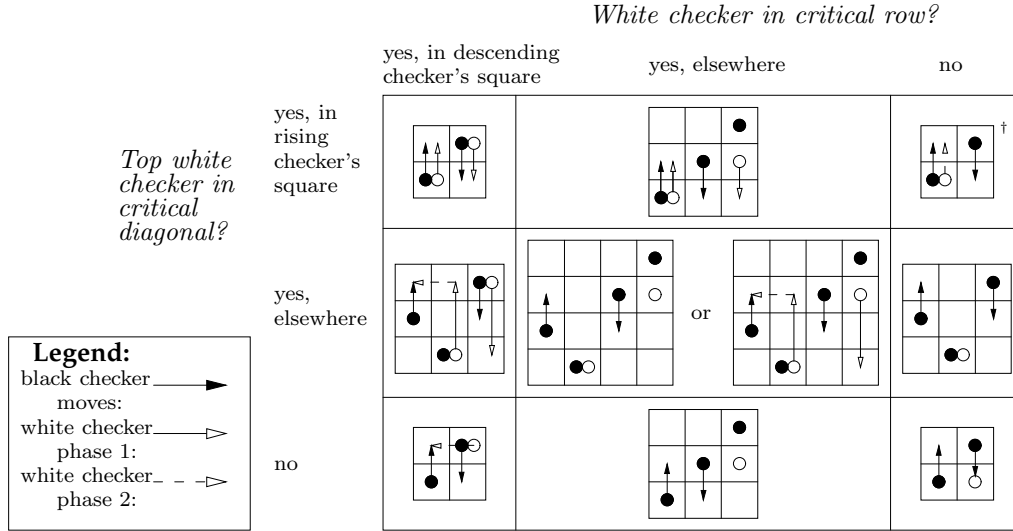


FIGURE 5. Examples of the nine cases (case \dagger is discussed in Sect. 2.6)

Littlewood-Richardson rules give combinatorial descriptions of Littlewood-Richardson coefficients $c_{\alpha\beta}^{\gamma}$, defined by

$$s_{\alpha}s_{\beta} = \sum_{\gamma} c_{\alpha\beta}^{\gamma} s_{\gamma}$$

where α and β are partitions, and s_{\cdot} are Schur functions. The checker games will compute the sum on the right modulo the ideal (in the ring of symmetric functions) defining the cohomology ring of the Grassmannian $G(k, n)$.

More precisely, let $Rec_{k,n-k}$ be the set of subdiagrams of the rectangle with k rows and $n - k$ columns. Throughout this article, we identify $Rec_{k,n-k}$ with subsets of $\{1, \dots, n\}$ of size k using the well-known bijection (see Figure 8). Fix α and β .

2.5. Theorem (Geometric Littlewood-Richardson rule, first version). —

- (a) $\sum_{\text{games } G} s_{\text{output}(G)} = \sum_{\gamma \in Rec_{k,n-k}} c_{\alpha\beta}^{\gamma} s_{\gamma}$, where the left sum is over all checker games with input α and β , and $\text{output}(G)$ is the output of checker game G .
- (b) Hence if $\gamma \in Rec_{k,n-k}$, then the integer $c_{\alpha\beta}^{\gamma}$ is the number of checker games starting with configuration $\circ_{\alpha,\beta} \bullet_{\text{init}}$ and ending with configuration $\circ_{\gamma} \bullet_{\text{final}}$.

For example, Figure 6 computes $s_{(1)}^2 = s_{(2)} + s_{(1,1)}$. Figure 7 computes $c_{(2,1),(2,1)}^{(3,2,1)} = 2$ using $k = 3, n = 6$.

Theorem 2.5 follows immediately from Theorem 3.9 (Geometric Littlewood-Richardson rule, second version).

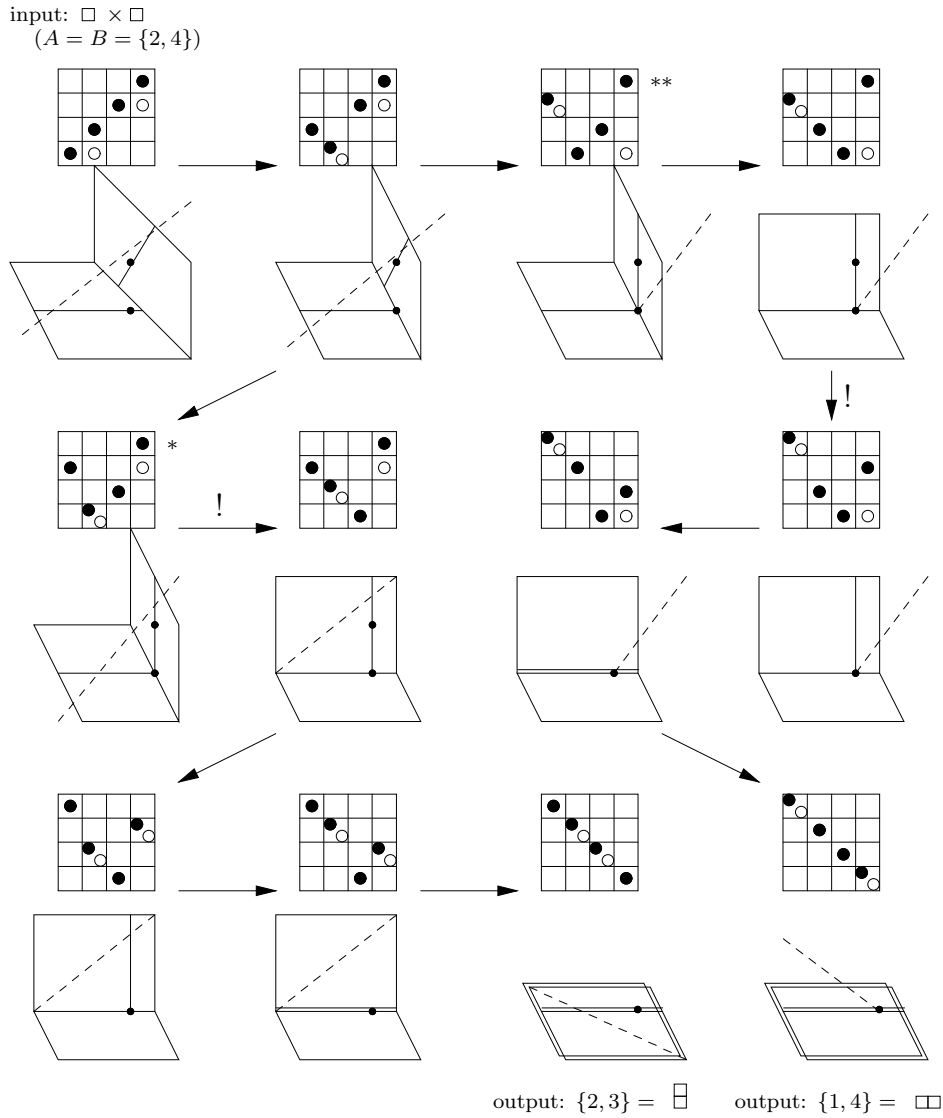


FIGURE 6. Two checker games with the same starting position, and the geometric interpretation of Section 3 (compare to Figure 2; checker configurations * and ** are discussed in Sect. 3.12, and the moves labeled “!” are discussed in Sect. 2.6)

2.6. Bijection to tableaux. There is a straightforward bijection to tableaux (using the tableaux description of [F, Cor. 5.1.2]). Whenever there is a move described by a † in Figure 5 (see also Table 2), where the “rising” white checker is the r^{th} white checker (counting by row) and the c^{th} (counting by column), place an r in row c of the tableau.

For example, in Figure 6, the left-most output corresponds to the (one-cell) tableau “2”, and the right-most output corresponds to the tableau “1”. The moves where the tableaux are filled are marked with “!”.

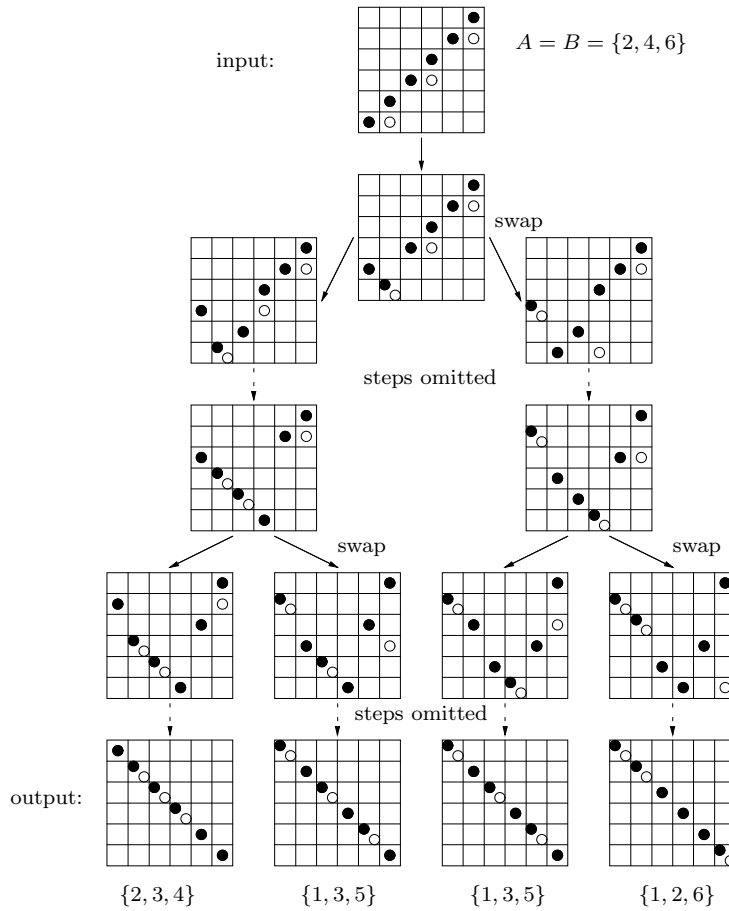


FIGURE 7. Computing $c_{(2,1),(2,1)}^{(3,2,1)} = 2$ using $k = 3, n = 6$; some intermediate steps are omitted

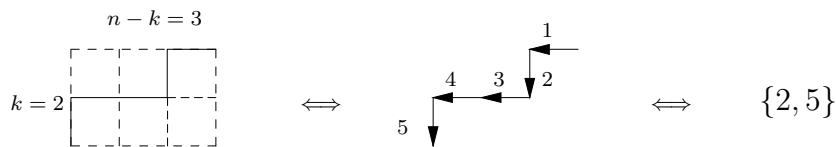


FIGURE 8. The bijection between $Rec_{k,n-k}$ and size k subsets of $\{1, \dots, n\}$

2.7. Remarks. (a) Like Pieri's formula and Monk's formula, this rule most naturally gives all terms in an intersection all at once (part (a)), but the individual coefficients can be easily extracted (part (b)).

(b) A derivation of Pieri's formula from the Geometric Littlewood-Richardson rule is left as an exercise to the reader. Note that Pieri's original proof was also by degeneration methods.

(c) Some properties of Littlewood-Richardson coefficients clearly follow from the Geometric Littlewood-Richardson rule, while others do not. For example, it is not clear why $c_{\alpha\beta}^\gamma = c_{\beta\alpha}^\gamma$. However, it can be combinatorially shown (most easily via the link to puzzles, Sect. 7) that (i) the rule is independent of the choice of n and k (i.e. the computation of $c_{\alpha\beta}^\gamma$ is independent of any n and k such that $\gamma \in Rec_{k,n-k}$), and (ii) the “trianlity” $c_{\alpha\beta}^\gamma = c_{\beta\gamma}^{\alpha^\vee}$ for $\alpha, \beta, \gamma \in Rec_{k,n-k}$ holds.

(d) We will need the following combinatorial observation.

2.8. Lemma. — Suppose at some point in the algorithm, the descending checker is in column c . Suppose the white checkers are at $(r_1, c_1), \dots, (r_k, c_k)$ with $c_1 < \dots < c_k$. Then (r_1, \dots, r_k) is increasing for $c_i \leq c$ and decreasing for $c_i \geq c$.

This follows from a straightforward induction showing that this property is preserved by each move. We say that configuration $\circ\bullet$ with this property is *mid-sort*. For example, the white checkers of Figures 7 and 21 are mid-sort.

3. DESCRIBING THE GEOMETRY OF THE GRASSMANNIAN AND FLAG VARIETY WITH CHECKERS

In this section, we interpret checker configurations geometrically, and state the main technical result of the paper, Theorem 3.10 (the Geometric Littlewood-Richardson rule, final version). Black checkers will correspond to the relative position of the two flags M and F , and white checkers will correspond to the position of the k -plane relative to the flags.

3.1. The relative position of two flags, given by black checkers; the variety X_\bullet . Given two flags M and F , construct an $n \times n$ “rank” table of the numbers $\dim M_i \cap F_j$. Up to the action of $GL(n)$, the two flags are specified by this table.

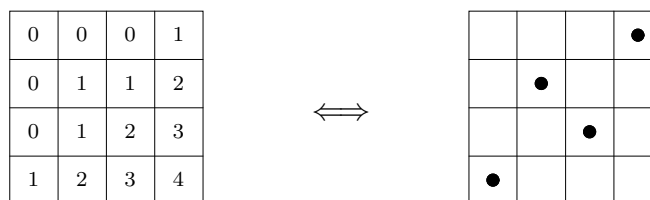


FIGURE 9. The relative position of two flags, given by numbers on an $n \times n$ board, and by a configuration of black checkers

This data is equivalent to the data of n black checkers on the checkerboard such that no two are in the same row or column. The bijection is given as follows. We say a square (i_1, j_1) *dominates* another square (i_2, j_2) if $i_1 \geq i_2$ and $j_1 \geq j_2$. Given the black checkers, $\dim M_i \cap F_j$ is given by the number of black checkers dominated by square (i, j) . An example of the bijection is given in Figure 9.

Note that each square in the table corresponds to a vector space, whose dimension is the number of black checkers dominated by that square. The vector space is the span of the vector spaces corresponding to the black checkers it dominates.

Let X_\bullet be the (locally closed) subvariety of $Fl(n) \times Fl(n)$ corresponding to flags (M, F) in relative position given by black checker configuration \bullet . The variety X_\bullet is smooth, and its codimension in $Fl(n) \times Fl(n)$ is the number of pairs of distinct black checkers a and b such that a dominates b . (This is a straightforward exercise; it also follows quickly from Sect. 5.) This sort of construction is common in the literature.

3.2. Side remark: Schubert varieties of the flag variety. For a fixed F and fixed configuration \bullet of black checkers, the set of M in $Fl(n)$ such that the relative position of M and F is given by \bullet is an open Schubert cell Ω_\bullet° (i.e. the second projection $pr_2 : X_\bullet \rightarrow Fl(n)$ is a fibration by Schubert cells). This set is a GL_n -orbit (what some authors call a “double Schubert cell”). Schubert cells are usually indexed by permutations; the bijection between checker configurations and permutations was given in Section 2.2. For example, the permutation corresponding to Figure 9 is 1324.

3.3. The specialization order. Given a point p of $Fl(n)$ (parametrizing M) in the dense open Schubert cell (with respect to a fixed reference flag F), the specialization order (Sect. 2.2) can be interpreted as a sequence in $Fl(n)$, consisting of a chain of $\binom{n}{2}$ \mathbb{P}^1 's, starting at p and ending with the “most degenerate” point of $Fl(n)$ (corresponding to the reference flag F).

We first describe the chain informally. Each \mathbb{P}^1 corresponds to a move of black checkers. All but one point of the \mathbb{P}^1 lies in one open stratum X_\bullet ; the remaining point (where the \mathbb{P}^1 meets the next component of the one-parameter degeneration) lies on an open stratum $X_{\bullet_{\text{next}}}$ of dimension one lower. If the move corresponds to the descending checker in row r dropping one row (and another checker to the left rising one row), then all components of the flags F and M except M_r are held fixed. For example, the geometry corresponding to the specialization order for $n = 4$ is shown in Figure 2.

More precisely, there is a \mathbb{P}^1 -fibration $X_\bullet \cup X_{\bullet_{\text{next}}} \rightarrow X_{\bullet_{\text{next}}}$; the \mathbb{P}^1 corresponding to a point of X_\bullet described in the previous paragraph is a fiber. A useful alternate description of $X_\bullet \cup X_{\bullet_{\text{next}}}$ is given in Section 5.6.

3.4. The position of a k -plane relative to two given flags, in terms of white checkers; two-flag Schubert varieties $Y_{\bullet\bullet}$ and $X_{\bullet\bullet}$. Suppose two flags M and F are in relative position given by black checker configuration \bullet . The position of a k -plane V relative to the two flags, up to the action of the subgroup of $GL(n)$ fixing the two flags, is determined by the table of numbers $\dim V \cap M_i \cap F_j$.

This data is equivalent to the data of k white checkers on the checkerboard that are happy (see Sect. 2.3), with no two in the same row or column. The bijection is given as follows: $\dim V \cap M_i \cap F_j$ is the number of white checkers in squares dominated by (i, j) . See Figure 6 for example; the line $\mathbb{P}V$ is depicted as a dashed line.

If \mathbf{M} . and \mathbf{F} . are two flags whose relative position is given by \bullet , let the *open two-flag Schubert variety* $Y_{\bullet\bullet} \subset G(k, n)$ be the set of k -planes whose position relative to the flags is given by $\circ\bullet$; define the *closed two-flag Schubert variety* $\overline{Y}_{\bullet\bullet}$ to be $\text{Cl}_{G(k, n)} Y_{\bullet\bullet}$. Let $X_{\bullet\bullet}$ (resp. $\overline{X}_{\bullet\bullet}$) in $G(k, n) \times X_{\bullet}$ be the *universal open* (resp. *closed*) *two-flag Schubert variety*. (Similar constructions are common in the literature.)

Note that (i) $X_{\bullet\bullet} \rightarrow X_{\bullet}$ is a $Y_{\bullet\bullet}$ -fibration; (ii) $\overline{X}_{\bullet\bullet} \rightarrow X_{\bullet}$ is an $\overline{Y}_{\bullet\bullet}$ -fibration, and proper; (iii) $G(k, n)$ is the disjoint union of the $Y_{\bullet\bullet}$ (for fixed \bullet and \mathbf{F} ., \mathbf{M} .); (iv) $G(k, n) \times \text{Fl}(n) \times \text{Fl}(n)$ is the disjoint union of the $X_{\bullet\bullet}$. *Caution*: the disjoint unions of (iii) and (iv) are not in general stratifications; Section 3.12 (a) provides a counterexample.

3.5. Lemma. — *The variety $Y_{\bullet\bullet}$ is irreducible and smooth; its dimension is the sum over all white checkers w of the number of black checkers w dominates minus the number of white checkers w dominates (including itself).*

The proof is straightforward and hence omitted.

3.6. Proposition (Initial position of white checkers). — *Suppose $A = \{a_1, \dots, a_k\}$ and $B = \{b_1, \dots, b_k\}$ are two subsets of $\{1, \dots, n\}$ of size k , and \mathbf{M} . and \mathbf{F} . are two transverse (opposite) flags (i.e. with relative position given by \bullet_{init}). Then $\Omega_A(\mathbf{M}.) \cap \Omega_B(\mathbf{F}.)$ is the closed two-flag Schubert variety $\overline{Y}_{\circ_{A, B} \bullet_{\text{init}}}$.*

In the literature, these intersections are known as *Richardson varieties* [R]; see [KL] for more discussion and references. They were also called *skew Schubert varieties* by Stanley [St1].

Proof. We deal first with the case of characteristic 0. By the Kleiman-Bertini theorem [K11], $\Omega_A(\mathbf{M}.) \cap \Omega_B(\mathbf{F}.)$ is reduced of the expected dimension. The generic point of any of its components lies in $Y_{\circ_1 \bullet_{\text{init}}}$ for some configuration \circ_1 of white checkers, where the first coordinates of the white checkers of \circ_1 are given by the set A and the second coordinates are given by the set B . A short calculation using Lemma 3.5 yields $\dim Y_{\circ_1 \bullet_{\text{init}}} \leq \dim Y_{\circ_{A, B} \bullet_{\text{init}}}$, with equality holding if and only if $\circ_1 = \circ_{A, B}$. (Reason: the sum over all white checkers w in \circ_1 of the number of black checkers w dominates is $\sum_{a \in A} a + \sum_{b \in B} b - kn$, which is independent of \circ_1 , so $\dim Y_{\circ_1 \bullet_{\text{init}}}$ is maximized when there is no white checker dominating another, which is the definition of $\circ_{A, B}$.) Then it can be checked directly that $\dim Y_{\circ_{A, B} \bullet_{\text{init}}} = \dim \Omega_A \cap \Omega_B$. As $Y_{\circ_{A, B} \bullet_{\text{init}}}$ is irreducible, the result in characteristic 0 follows.

In positive characteristic, the same argument shows that the cycle $\Omega_A(\mathbf{M}.) \cap \Omega_B(\mathbf{F}.)$ is some positive multiple of the the cycle $\overline{Y}_{\circ_{A, B} \bullet_{\text{init}}}$. It is an easy exercise to show that the intersection is transverse, i.e. that this multiple is 1. It will be easier still to conclude the proof combinatorially; we will do this in Section 3.11.

3.7. The Geometric Littlewood-Richardson rule: deforming cycles in the Grassmannian. We can now give a geometric interpretation of Theorem 2.5 (which will be the first version of the Geometric Littlewood-Richardson rule). We wish to compute the class (in $H_*(G(k, n))$) of the intersection of two Schubert cycles. By the Kleiman-Bertini theorem

[K11] (or our Grassmannian Kleiman-Bertini theorem [V2, Thm. 2.6] in positive characteristic), this is the class of the intersection of two Schubert varieties with respect to two general (transverse) flags, which by Proposition 3.6 is $[\overline{Y}_{\circ_{A,B}\bullet\text{init}}]$. By a sequence of codimension 1 degenerations (corresponding to the specialization order), we degenerate the two flags until they are equal. The base of each degeneration is a \mathbb{P}^1 in $Fl(n)$, where $\mathbb{A}^1 \subset X_\bullet$ and $\{\infty\} \in X_{\bullet\text{next}}$. We have a $\overline{Y}_{\circ\bullet}$ -fibration above \mathbb{A}^1 . The fiber above ∞ of the closure of this fibration (in $G(k, n) \times \mathbb{P}^1$) turns out to be one of $\overline{Y}_{\circ_{\text{stay}}\bullet\text{next}}$, $\overline{Y}_{\circ_{\text{swap}}\bullet\text{next}}$, or $\overline{Y}_{\circ_{\text{stay}}\bullet\text{next}} \cup \overline{Y}_{\circ_{\text{swap}}\bullet\text{next}}$ (Theorem 3.9; \circ_{stay} and \circ_{swap} were defined in Sect. 2.3); the components appear with multiplicity 1. In other words, the two-flag Schubert variety degenerates to another two-flag Schubert variety, or to the union of two. Figure 6 illustrates the geometry behind the computation of $s_{(1)}^2 = s_{(1,1)} + s_{(2)}$ in $G(2, 4)$.

3.8. More precisely, assume the black checker configuration \bullet is in the specialization order, and the white checkers are *mid-sort* (in the sense of Lemma 2.8). Consider the diagram:

$$(1) \quad \begin{array}{ccccc} \overline{X}_{\circ\bullet} := \text{Cl}_{G(k,n) \times X_\bullet} X_{\circ\bullet} & \hookrightarrow & \text{Cl}_{G(k,n) \times (X_\bullet \cup X_{\bullet\text{next}})} X_{\circ\bullet} & \hookrightarrow & D_X \\ \downarrow & & \downarrow & & \downarrow \\ X_\bullet & \hookrightarrow & X_\bullet \cup X_{\bullet\text{next}} & \hookrightarrow & X_{\bullet\text{next}} \end{array}$$

The Cartier divisor D_X is defined by fibered product. Note that the vertical morphisms are proper, the vertical morphism on the left is a $\overline{Y}_{\circ\bullet}$ -fibration, the horizontal inclusions on the left are open immersions, and the horizontal inclusions on the right are closed immersions.

The geometric constructions described in Section 3.7 are obtained from (1) by base changing via $\mathbb{P}^1 \rightarrow X_\bullet \cup X_{\bullet\text{next}}$ (described in Sect. 3.3), to obtain:

$$(2) \quad \begin{array}{ccccc} \mathcal{Y}_{\circ\bullet} & \hookrightarrow & \text{Cl}_{G(k,n) \times \mathbb{P}^1} \mathcal{Y}_{\circ\bullet} & \hookrightarrow & D_Y \\ \downarrow & & \downarrow & & \downarrow \\ \mathbb{A}^1 & \hookrightarrow & \mathbb{P}^1 & \hookrightarrow & \{\infty\} \end{array}$$

Here $\mathcal{Y}_{\circ\bullet}$, $\text{Cl}_{G(k,n) \times \mathbb{P}^1} \mathcal{Y}_{\circ\bullet}$, and D_Y are defined by fibered product (or restriction) from (1). Again, the vertical morphisms are proper, the vertical morphism on the left is a $\overline{Y}_{\circ\bullet}$ -fibration, the horizontal inclusions on the left are open immersions, and the horizontal inclusions on the right are closed immersions.

The informal statement of Section 3.7 can now be made precise:

3.9. Theorem (Geometric Littlewood-Richardson rule, second version). — $D_Y = \overline{Y}_{\circ_{\text{stay}}\bullet\text{next}}$, $\overline{Y}_{\circ_{\text{swap}}\bullet\text{next}}$, or $\overline{Y}_{\circ_{\text{stay}}\bullet\text{next}} \cup \overline{Y}_{\circ_{\text{swap}}\bullet\text{next}}$.

By base change from (1) to (2), Theorem 3.9 is a consequence of the following, which is proved in Section 6. (The notation $\mathcal{Y}_{\circ\bullet}$ and D_Y will not be used hereafter.)

3.10. Theorem (Geometric Littlewood-Richardson rule, final version). — $D_X = \overline{X}_{\circ_{\text{stay}}\bullet\text{next}}$, $\overline{X}_{\circ_{\text{swap}}\bullet\text{next}}$, or $\overline{X}_{\circ_{\text{stay}}\bullet\text{next}} \cup \overline{X}_{\circ_{\text{swap}}\bullet\text{next}}$.

In other words, a particular divisor D_X (corresponding to $X_{\bullet_{\text{next}}} \subset X_{\bullet} \cup X_{\bullet_{\text{next}}}$) on a universal two-flag Schubert variety is another such variety, or the union of two such varieties.

3.11. Enumerative problems and checker tournaments. Suppose $\Omega_{\alpha_1}, \dots, \Omega_{\alpha_\ell}$ are Schubert classes on $G(k, n)$ of total codimension $\dim G(k, n)$. Then (the degree of) their intersection — the solution to an enumerative problem by the Kleiman-Bertini theorem [K11] (or our Grassmannian Kleiman-Bertini theorem [V2, Thm. 2.6] in positive characteristic) — can clearly be inductively computed using the Geometric Littlewood-Richardson rule. Hence Schubert problems can be solved by counting *checker tournaments* of $\ell - 1$ games, where the input to the first game is α_1 and α_2 , and for $i > 1$ the input to the i^{th} game is α_{i+1} and the output of the previous game. (The outcome of each checker tournament will always be the same — the class of a point.)

Conclusion of proof of Proposition 3.6 in positive characteristic. We will show that the multiplicity with which $\overline{Y}_{\circ_{A,B}\bullet_{\text{init}}}$ appears in $\Omega_A(\mathbf{M}) \cap \Omega_B(\mathbf{F})$ is 1. (We will not use the Grassmannian Kleiman-Bertini Theorem [V2, Thm. 2.6] as its proof relies on Prop. 3.6.)

Choose $C = \{c_1, \dots, c_k\}$ such that $\dim \Omega_A \cup \Omega_B \cup \Omega_C = 0$ (where \cup is the cup product in cohomology) and $\deg \Omega_A \cup \Omega_B \cup \Omega_C > 0$. In characteristic 0, the above discussion shows that $\deg \Omega_A \cup \Omega_B \cup \Omega_C$ is the number of checker tournaments with inputs A, B, C . In positive characteristic, the above discussion shows that if the multiplicity is greater than one, then $\deg \Omega_A \cup \Omega_B \cup \Omega_C$ is *strictly less* than the same number of checker games. But $\deg \Omega_A \cup \Omega_B \cup \Omega_C$ is independent of characteristic, yielding a contradiction. \square

3.12. Cautions. (a) The degenerations used in the Geometric Littlewood-Richardson rule follow the specialization order. An arbitrary path through the Bruhat order will not work in general. For example, if $\circ\bullet$ is as shown on the left of Figure 10, then $X_{\circ\bullet}$ corresponds to points p_1 and p_2 in \mathbb{P}^3 , lines ℓ_1 and ℓ_2 through p_1 such that ℓ_1, ℓ_2 , and p_2 span \mathbb{P}^3 , and a point $q \in \ell_1 - p_1$. Then for example $\mathbf{M}_3 = \text{span}(\ell_2, p_2)$ and the line corresponding to the point of $G(2, 4)$ is $\text{span}(q, p_2)$. The degeneration shown in Figure 10 (to \bullet' , say) corresponds to letting p_2 tend to p_1 , and remembering the line ℓ_3 of approach. Then the divisor on $\text{Cl}_{G(k,n) \times (X_{\bullet} \cup X_{\bullet_{\text{next}}})} X_{\circ\bullet}$ corresponding to $X_{\bullet'}$ parametrizes lines through p_1 contained in $\text{span}(\ell_1, \ell_3)$; this is not of the form $X_{\circ'\bullet'}$ for any \circ' .

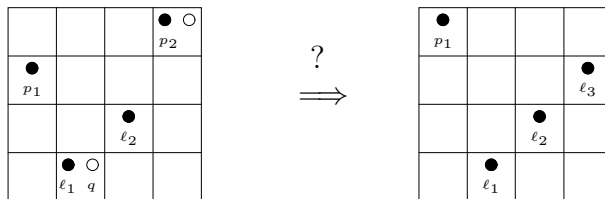


FIGURE 10. The dangers of straying from the specialization order

(b) Unlike the variety $\overline{X}_\bullet = \text{Cl}_{Fl(n) \times Fl(n)} X_\bullet$, the variety $\overline{X}_{\circ\bullet}$ cannot be defined numerically, i.e. in general $\overline{X}_{\circ\bullet}$ will be only one irreducible component of

$$X'_{\circ\bullet} := \{(V, \mathbf{F}, \mathbf{M}) \in G(k, n) \times X_\bullet \subset G(k, n) \times Fl(n) \times Fl(n) : \dim V \cap \mathbf{F}_i \cap \mathbf{M}_j \geq \gamma_{\circ\bullet}^{i,j}\}$$

where $\gamma_{\circ\bullet}^{i,j}$ is the number of white checkers dominated by (i, j) . For example, in Figure 6, if $\circ\bullet$ is the configuration marked “*” and $\circ'\bullet$ is the configuration marked “**”, then $X'_{\circ\bullet} = \overline{X}_{\circ\bullet} \cup \overline{X}_{\circ'\bullet}$.

4. APPLICATION: LITTLEWOOD-RICHARDSON RULES

In this section, we discuss the bijection between checkers, the classical Littlewood-Richardson rule involving tableaux, and puzzles. We extend the checker and puzzle rules to K -theory, proving a conjecture of Buch. (We rely on Buch’s extension of the tableau rule [B1].) We then describe progress of extending this method to the flag manifold (the open question of a Littlewood-Richardson rule for Schubert polynomials). Finally, we conclude with open questions.

4.1. Checkers, puzzles, tableaux. A bijection between checker games and puzzles is given in Section 7. Combining this with Tao’s “proof-without-words” of a bijection between puzzles and tableaux (given in Figure 11) yields the bijection between checker-games and tableaux:

4.2. Theorem (bijection from checker games to tableaux). — *The construction of Section 2.6 gives a bijection from checker games to tableaux.*

There is undoubtedly a simpler direct proof (given the elegance of this map, and the inelegance of the bijection from checkers to puzzles).

Hence checker games give the first geometric interpretation of tableaux and puzzles; indeed there is a bijection between tableaux/puzzles and solutions of the corresponding triple-intersection Schubert problem, once branch paths are chosen [V2, Sect. 4.3], [SVV].

Note that to each puzzle, there are three possible checker-games, depending on the orientation of the puzzle. These correspond to three degenerations of three general flags. It would be interesting to relate these three degenerations.

4.3. K -theory: checkers, puzzles, tableaux. Buch [B2] has conjectured that checker-game analysis can be extended to K -theory or the Grothendieck ring (see [B1] for background on the K -theory of the Grassmannian). Precisely, the rules for checker moves are identical, except there is a new term in the middle square of Table 2 (the case where there is a choice of moves), of one lower dimension, with a minus sign. If the two white checkers in question are at (r_1, c_1) and (r_2, c_2) , with $r_1 > r_2$ and $c_1 < c_2$, then they move to (r_2, c_1) and $(r_1 - 1, c_2)$ (see Figure 12). Call this a *sub-swap*; denote the resulting configuration $\circ_{\text{sub}}\bullet_{\text{next}}$. Note that by Lemma 3.5, $\dim \overline{Y}_{\circ_{\text{sub}}\bullet_{\text{next}}} = \dim \overline{Y}_{\circ\bullet} - 1$.

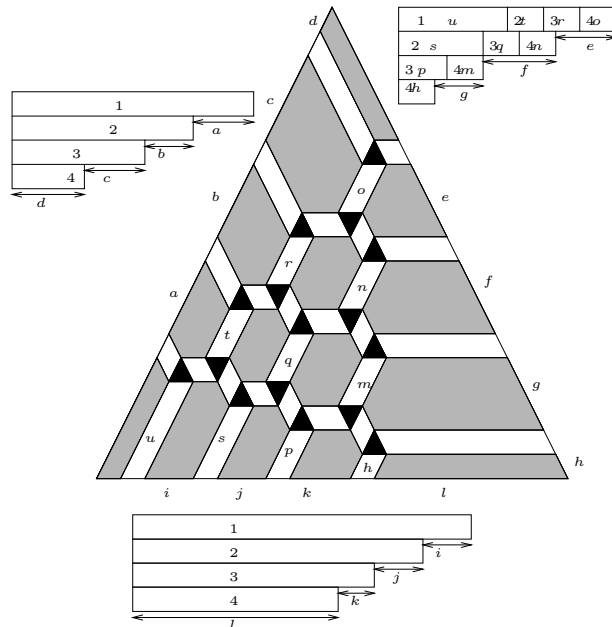


FIGURE 11. Tao’s “proof without words” of the bijection between puzzles and tableaux (1-triangles are depicted as black, regions of 0-rectangles are grey, and regions of rhombi are white)

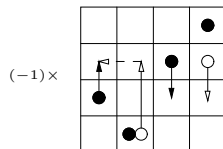


FIGURE 12. Buch’s “sub-swap” case for the K -theory geometric Littlewood-Richardson rule (cf. Figure 5)

4.4. Theorem (K -theory Geometric Littlewood-Richardson rule). — *Buch’s rule describes multiplication in the Grothendieck ring of $G(k, n)$.*

Proof. We give a bijection from K -theory checker games to Buch’s “set-valued tableaux” (certain tableaux whose entries are sets of consecutive integers, [B1]), generalizing the bijection of Section 2.6. Each white checker now has a memory of certain earlier rows. Each time there is a sub-swap, where a checker rises from being the r^{th} white checker to being the $(r - 1)^{\text{st}}$ (counting by row), that checker adds to its memory that it had once been the r^{th} checker (by row). Whenever there is move described by a \dagger in Figure 5, where the white checker is the r^{th} by row and the c^{th} by column, in row c of the tableau place the set consisting of r and all remembered earlier rows. Then erase the memory of that white checker. (The reader may verify that in Figure 6 ($G(2, 4)$), the result is an additional set-valued tableau, with a single cell containing the set $\{1, 2\}$.)

The proof that this is a bijection is straightforward and left to the reader. □

This result suggests that Buch’s rule reflects a geometrically stronger fact, extending the final version of the Geometric Littlewood-Richardson rule 3.10.

4.5. Conjecture (*K-theory Geometric Littlewood-Richardson rule, geometric form, with A. Buch*).
—

- (a) *In the Grothendieck ring, $[X_{\bullet\bullet}] = [\overline{X}_{\circ_{stay}\bullet_{next}}], [\overline{X}_{\circ_{swap}\bullet_{next}}],$ or $[\overline{X}_{\circ_{stay}\bullet_{next}}] + [\overline{X}_{\circ_{swap}\bullet_{next}}] - [\overline{X}_{\circ_{sub}\bullet_{next}}].$*
- (b) *Scheme-theoretically, $D_X = \overline{X}_{\circ_{stay}\bullet_{next}}, \overline{X}_{\circ_{swap}\bullet_{next}},$ or $\overline{X}_{\circ_{stay}\bullet_{next}} \cup \overline{X}_{\circ_{swap}\bullet_{next}}.$ In the latter case, the scheme-theoretic intersection $\overline{X}_{\circ_{stay}\bullet_{next}} \cap \overline{X}_{\circ_{swap}\bullet_{next}}$ is a translate of $\overline{X}_{\circ_{sub}\bullet_{next}}.$*

Part (a) clearly follows from part (b).

Knutson has speculated that the total space of the degeneration is Cohen-Macaulay; this would imply the conjecture.

The *K*-theory Geometric Littlewood-Richardson rule 4.4 can be extended to puzzles.

4.6. Theorem (*K-theory Puzzle Littlewood-Richardson rule*). — *The K-theory Littlewood-Richardson coefficient corresponding to subsets α, β, γ is the number of puzzles with sides given by α, β, γ completed with the pieces shown in Figure 13. There is a factor of -1 for each K-theory piece in the puzzle.*

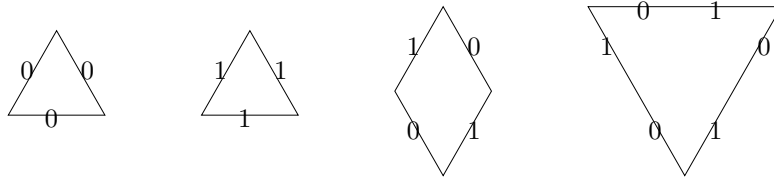


FIGURE 13. The *K*-theory puzzle pieces

The first three pieces of Figure 13 are the usual puzzle pieces of [KTW, KT]; they may be rotated. The fourth piece is new; it may not be rotated. Tao had earlier, independently, discovered this piece [T].

Theorem 4.6 may be proved via the *K*-theory Geometric Littlewood-Richardson rule 4.4, or by generalizing Tao’s proof of Figure 11. Both proofs are omitted.

As a consequence, we immediately have:

4.7. Corollary (*triatlity of K-theory Littlewood-Richardson coefficients*). — *If K-theory Littlewood-Richardson coefficients are denoted $C_{\cdot\cdot}, C_{\alpha\beta}^{\gamma\vee} = C_{\beta\gamma}^{\alpha\vee} = C_{\gamma\alpha}^{\beta\vee}.$*

This is immediate in cohomology, but not obvious in the Grothendieck ring. The following direct proof is due to Buch (cf. [B1, p. 30]).

Proof. Let $\rho : G(d, n) \rightarrow pt$ be the map to a point. Define a pairing on $K_0(X)$ by $(a, b) := \rho_*(a \cdot b)$. This pairing is perfect, but (unlike for cohomology) the Schubert structure sheaf basis is not dual to itself. However, if t denotes the top exterior power of the tautological subbundle on $G(k, n)$, then the dual basis to the structure sheaf basis is

$$\{t\mathcal{O}_Y : Y \text{ is a Schubert variety in } G(k, n)\}.$$

More precisely, the structure sheaf for a partition $\lambda = (\lambda_1, \dots, \lambda_k)$ is dual to t times the structure sheaf for $\lambda^\vee = (n - k - \lambda_k, \dots, n - k - \lambda_1)$. (For more details, see [B1, Sect. 8]; this property is special for Grassmannians.) Hence $\rho_*(t\mathcal{O}_\lambda \mathcal{O}_\mu \mathcal{O}_n u) = C_{\lambda\mu}^{\nu^\vee} = C_{\mu\nu}^{\lambda^\vee} = C_{\nu\lambda}^\mu$. \square

4.8. Toward a Geometric Littlewood-Richardson rule for flag manifolds. The same methods can be applied to flag manifolds, in the hope of addressing the important open problem of finding a Littlewood-Richardson rule in this context (i.e. structure coefficients for the multiplication of Schubert polynomials), see [St2], [F, p. 180], [FP, Sect. 9.10]. This problem has already motivated a great deal of remarkable work.

We describe some partial results here, informally. Define two-flag Schubert varieties X_δ of flag manifolds analogously to $X_{\bullet\bullet}$, as the locus in $Fl(n) \times Fl(n) \times Fl(n)$ parametrizing (i) two flags \mathbf{F} and \mathbf{M} in relative position given by \bullet , and (ii) a third flag F such that $\dim \mathbf{F}_i \cap \mathbf{M}_j \cap F_k = \delta_{ijk}$. The configuration \bullet is obtained from the rank table $(\delta_{ijn})_{i,j}$ by the bijection of Section 3.1. The choice of the data δ_{ijk} for which this data is non-empty can be usefully summarized in two (equivalent) ways. It is not yet clear which is the more convenient notation.

First, these δ correspond to configurations of checkers on an $n \times n$ board, where there are i checkers labeled i for $1 \leq i \leq n$. No two checkers with the same label are in the same column or the same row. An i -checker ($i < n$) is *happy* if there is an $(i + 1)$ -checker to its left (or in the same square) and an $(i + 1)$ -checker above it (or in the same square). (See for example Figure 14.) The bijection to δ is given as follows: δ_{ijk} is the number of k -checkers dominated by (i, j) . The morphism to X_\bullet corresponds to forgetting all but the n -checkers.

Second, these δ correspond to “wiring diagrams”, with n wires entering the board from below and leaving the board on the right. The bijection to δ is given as follows: δ_{ijk} is the number of wires numbered at least k dominated by (i, j) . See Figure 15 for an example.

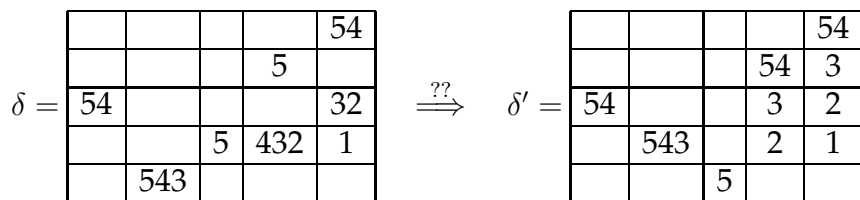


FIGURE 14. Is the two-flag Schubert variety on the right in the closure of the one on the left?

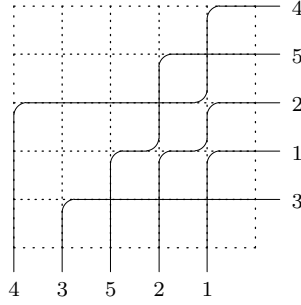


FIGURE 15. The “wiring diagram” corresponding to the first checker configuration of Figure 14

There is an analogue of Proposition 3.6, describing the intersection of two Schubert varieties (with respect to transverse flags F and M) as \overline{X}_δ for an explicitly given δ ; call the set of δ obtained in such a way the *initial positions*.

4.9. Conjecture (Existence of a Geometric Littlewood-Richardson rule for flag manifolds). — *There exists a subset M of the $\{(\delta_{ijk})_{ijk}\}$, where the configuration of n -checkers is in the specialization order (analogous to “mid-sort”), containing the set of initial positions, such that the divisor D_X on \overline{X}_δ corresponding to the next element of the specialization order is the union of varieties of the form $\overline{X}_{\delta'}$, each appearing with multiplicity 1, where $(\delta'_{ijk})_{ijk} \in M$.*

This conjecture (which parallels Theorem 3.10) looks quite weak, as it specifies neither (i) the “mid-sort” property M nor (ii) how to determine δ' . However, it suffices to obtain almost all of the applications described in [V2] (e.g. reality, number of solutions in positive characteristic, numerical calculation of solutions to all Schubert problems, and more). Furthermore, it implies the existence of a Littlewood-Richardson rule, and an answer to (ii) would give an explicit rule.

4.10. Proposition. — *Conjecture 4.9 is true for $n \leq 5$.*

This is a considerable amount of evidence, involving $\sum_{n=1}^5 \binom{n}{2} \sum_{\alpha,\beta,\gamma} c_{\alpha\beta}^\gamma$ degenerations. However, there are two serious reasons to remain suspicious: (a) Knutson’s puzzle variant computes Littlewood-Richardson coefficients for $n < 5$ but fails for $n = 5$ (and puzzles are related to checkers via Sect. 7), and (b) all Littlewood-Richardson coefficients are 0 or 1 for $n < 6$.

Sketch of proof of Proposition 4.10 for $n \leq 4$. We build M inductively, starting with the set of initial positions. Successively, for each element δ of M , we find a list of possible divisors $\overline{X}_{\delta'}$ on \overline{X}_δ (above $X_{\bullet_{\text{next}}}$) as follows. If the n -checkers of δ are in position \bullet , the n -checkers of δ' are in position \bullet_{next} . Then given the positions of the k -checkers of δ and the $(k+1)$ -checkers of δ' (for $1 \leq k < n$), we list the (finite number of) possibilities of the choice of positions of the choices of k -checkers of δ' subject to two conditions: the k -checkers are happy, and $\delta'_{ijk} \geq \delta_{ijk}$. We then discard all δ' such that $\dim X_{\delta'} < \dim X_\delta - 1$.

Then each component of D_X lies in $D_{\delta'}$ for some remaining δ' . If any $X_{\delta'}$ has dimension at least $\dim X_{\delta}$, we stop, and the process fails. Otherwise, D_X must consist of a union of these $X_{\delta'}$, possibly with multiplicity. We then add these δ' to M . (This is a greedy algorithm, which sometimes includes δ' which do not correspond to components of D_X .) Thus the conjecture is true for this δ (with this choice of M) with the possible exception of the multiplicity 1 claim. We now repeat the process with this enlarged M .

For $n \leq 4$, one checks (most easily by computer) that this process never fails. Moreover, as all Littlewood-Richardson coefficients for $n \leq 4$ are 1, the multiplicity must be 1 at each stage. \square

The author has a full description of the degenerations which actually appear for $n \leq 4$, available upon request. However, it is not clear how to generalize this to a conjectural Littlewood-Richardson rule.

For $n = 5$, this process fails at six cases (where $\dim X_{\delta'} = \dim X_{\delta}$). However, in three of the six cases, it can be shown that \overline{X}_{δ} does not meet $X_{\delta'}$ (one is shown in Figure 14; the other two are identical except for the position of the 1-checker), and in the other three cases, δ itself can be removed from M (i.e. δ was falsely included in M by the greediness of the algorithm).

For larger n , this greedy algorithm will certainly produce even worse pathologies (i.e. arbitrarily many cases where $\dim X_{\delta'} - \dim X_{\delta}$ is arbitrarily large).

4.11. Questions. One motivation for the Geometric Littlewood-Richardson rule is that it should generalize well to other important geometric situations (as it has in K -theory and at least partially for the flag manifold). We now briefly describe some potential applications; some are work in progress.

(a) These methods may apply to other groups where Littlewood-Richardson rules are not known. For example, for the symplectic Grassmannian, there are only rules in the Lagrangian and Pieri cases. L. Mihalcea has made progress in finding a Geometric Littlewood-Richardson rule in the Lagrangian case, and has suggested that a similar algorithm should exist in general.

(b) An important intermediate stage between the Grassmannian and the full flag manifold is the two-step partial flag manifold. This case has useful applications, for example, to Grassmannians of other groups. The preprint [BKT] gives a connection to Gromov-Witten invariants (and does much more). The Littlewood-Richardson behavior of the two-step partial flag manifold is much better than for full flag manifolds. Buch, Kresch, and Tamvakis have suggested that Knutson's proposed partial flag rule (which fails for flags in general) holds for two-step flags, and have verified this up to $n = 16$ [BKT, p. 6].

Is there a good (and straightforward) checker-rule for such homogeneous spaces?

(c) Can equivariant Littlewood-Richardson coefficients be understood geometrically in this way? For example, can equivariant puzzles [KT] be translated to checkers, and can

partially-completed equivariant puzzles thus be given a geometric interpretation? Can this be combined with Theorem 4.4 to yield a Littlewood-Richardson rule in equivariant K -theory?

(d) The quantum cohomology of the Grassmannian can be translated into classical questions in the enumerative geometry of surfaces. One may hope that degeneration methods introduced here and in [V1] will apply. This perspective is being pursued (with different motivation) independently by I. Coskun (for rational scrolls), D. Avritzer, and M. Honsen (on Veronese surfaces).

(e) Is there any relation between the wiring diagrams of Figure 15 and rc-graphs? (We suspect not.)

(f) D. Eisenbud and J. Harris [EH] have a particular (irreducible, one-parameter) path in the flag variety, whose general point is in the large open Schubert cell, and whose special point is the smallest cell: consider the osculating flag M . to a point p on a rational normal curve, as p tends to a reference point q with osculating flag F . Eisenbud has asked if the specialization order is some sort of limit (a “polygonalization”) of such paths. This would provide a single path that breaks intersections of Schubert cells into their components. (Of course, the limit cycles could not have multiplicity one in general.) Eisenbud and Harris’ proof of the Pieri formula is evidence that this could be true.

Sottile has a precise conjecture generalizing Eisenbud and Harris’ approach to all flag manifolds [S3, Sect. 5]. He has generalized this further: one replaces the rational normal curve by the curve $e^{t\eta}X_u(F)$, where η is a principal nilpotent in the Lie algebra of the respective algebraic group, and the limit is then $\lim_{t \rightarrow 0} e^{t\eta}X_u(F) \cap X_w$, where X_w is given by the flag fixed by $\lim_{t \rightarrow 0} e^{t\eta}$, [S4]. Eisenbud’s question in this context then involves polygonalizing or degenerating this path.

5. BOTT-SAMELSON VARIETIES

5.1. We will associate a variety to the following data.

- n is a positive integer.
- \mathcal{P} is a finite subset of the plane (visualized so that downwards corresponds to increasing the first coordinate and rightwards corresponds to increasing the second coordinate, in keeping with the labeling convention for tables), with the partial order \prec given by domination (defined in Sect. 3.1).
- $\dim : \mathcal{P} \rightarrow \{0, 1, 2, \dots, n\}$ is a morphism of posets (i.e. weakly order-preserving map), denoted *dimension*.
- If $[a, b]$ is a covering relation (i.e. minimal interval) in \mathcal{P} (i.e. $a, b \in \mathcal{P}$, $a \prec b$, and there is no $c \in \mathcal{P}$ such that $a \prec c \prec b$), then $\dim a = \dim b - 1$. (This condition is likely unnecessary.)
- \mathcal{P} has a maximum element and a minimum element.

We call this data a *planar poset*, and denote it by \mathcal{P} ; the remaining data (\prec, \dim, n) will be implicit.

It will be convenient to represent this data as a planar graph, whose vertices are elements of \mathcal{P} , and whose edges correspond to covering relations in \mathcal{P} . The interior of the graph is a union of quadrilaterals; call these the *quadrilaterals of \mathcal{P}* . An element of \mathcal{P} at (i, j) is said to be on the *southwest border* (resp. *northeast border*) if there are no elements of \mathcal{P} (i', j') such that $i' \geq i$ and $j' \leq j$ (resp. $i' \leq i$ and $j' \geq j$); see Figure 16.

Define the *Bott-Samelson variety* $BS(\mathcal{P})$ to be the variety parametrizing a $(\dim s)$ -plane V_s in K^n for each $s \in \mathcal{P}$, with $V_s \subset V_t$ for $s \prec t$. (It is a closed subvariety of $\prod_{s \in \mathcal{P}} G(\dim s, n)$.) Elements s of \mathcal{P} will be written in bold-faced font; corresponding vector spaces will be denoted V_s .

Forgetting all but the vertices on the southwest border yields a morphism to the flag manifold, and the usual Bott-Samelson variety is a fiber of this morphism.

5.2. Lemma. — *The Bott-Samelson variety $BS(\mathcal{P})$ is smooth.*

Proof. Consider the planar graph representation of \mathcal{P} described above. The variety parametrizing the subspaces corresponding to the southwest border of the graph is a partial flag variety (and hence smooth). The Bott-Samelson variety $BS(\mathcal{P})$ can be expressed as a tower of \mathbb{P}^1 -bundles over the partial flag variety by inductively adding the data of elements of $s \in S$ corresponding to “new” vertices of quadrilaterals (where the other three vertices $s_1 \prec s_2 \prec s_3$ are already parametrized, and $s_1 \prec s \prec s_3$). \square

For example, Figure 16 illustrates that one particular Bott-Samelson variety is a tower of five \mathbb{P}^1 -bundles over $Fl(4)$; the correspondence of the \mathbb{P}^1 -bundles with quadrilaterals is illustrated by the arrows.

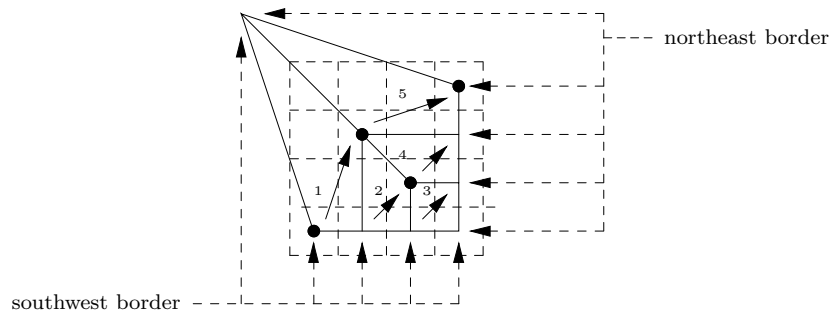


FIGURE 16. The northeast and southwest borders of a planar poset generated by a checker configuration; description of a Bott-Samelson variety as a tower of five \mathbb{P}^1 -bundles over $Fl(4)$

5.3. Strata of Bott-Samelson varieties. Any subset Q of the quadrilaterals of a planar poset determines a *stratum* of the Bott-Samelson variety. The closed stratum corresponds

to requiring the subspaces of the opposite corners of the quadrilaterals in Q of the same dimension to be the same. The open stratum corresponds to also requiring the spaces of the opposite corners of the quadrilaterals *not* in Q to be distinct. By the construction in the proof of Lemma 5.2, (i) the open strata give a stratification, (ii) the closed strata are smooth, and (iii) the codimension of the stratum is the size of the subset Q . It will be convenient to depict a stratum by placing an “=” in the quadrilaterals of Q , indicating the pairs of subspaces that are required to be equal (see for example Figure 17).

5.4. Example: planar posets generated by a set of checkers. Given a checker configuration \bullet (or \circ) and a positive integer n , we define the planar poset \mathcal{P}_\bullet (or \mathcal{P}_\circ) as follows. Include the squares of the table where there is a checker above (or possibly in the same square), and a checker to the left (or in the same square); include also a “zero element” above and to the left of the checkers. (The definition of happy in Sect. 2.3 can be rephrased as: the white checkers lie on elements of \mathcal{P}_\bullet .) For $s \in \mathcal{P}$, let $\dim s$ be the number of checkers dominated by s .

For example, if \bullet is a configuration of n checkers (as in Sect. 2.2), then the southwest border of \mathcal{P}_\bullet corresponds to \mathbf{F}_\bullet , and the northeast border corresponds to \mathbf{M}_\bullet ; $BS(\mathcal{P}_\bullet)$ is a fibration over $Fl(n)$ (where $Fl(n)$ parametrizes \mathbf{F}_\bullet), and the fiber is a Bott-Samelson resolution of $\Omega_\bullet(\mathbf{F}_\bullet)$. Figure 16 describes a Bott-Samelson resolution of the double Schubert variety corresponding to 1324. Similarly, the morphism $BS(\mathcal{P}_\bullet) \rightarrow \overline{X}_\bullet$ is a resolution of singularities. This morphism restricts to an isomorphism of the dense open stratum of $BS(\mathcal{P}_\bullet)$ with X_\bullet . If \bullet is in the specialization order, then $BS(\mathcal{P}_{\bullet_{\text{next}}})$ is (isomorphic to) a codimension 1 stratum of this Bott-Samelson variety. See Figure 17 for an example.

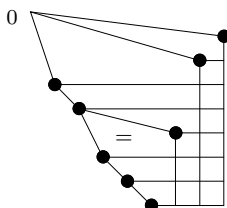


FIGURE 17. The poset corresponding to \bullet of Figure 3, with the divisorial stratum corresponding to \bullet_{next} marked with an “=”

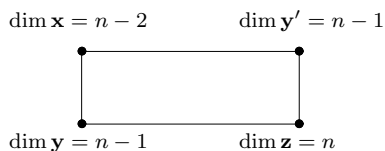


FIGURE 18. The planar poset \mathcal{P}_\square

5.5. Bott-Samelson varieties of morphisms of posets. Suppose \mathcal{P} and \mathcal{Q} are two planar posets (for the same n), and $p : \mathcal{P} \rightarrow \mathcal{Q}$ is a morphism of posets (i.e. a weakly

order-preserving map of sets, with no conditions on the planar structures). Then let $BS(p) = BS(\mathcal{P} \rightarrow \mathcal{Q})$ be the subvariety of $BS(\mathcal{P}) \times BS(\mathcal{Q})$ such that if $p(s) = t$, then the subspace corresponding to s is contained in the subspace corresponding to t . For example, a configuration of black and white checkers $\circ\bullet$ induces a morphism of posets $p_{\circ\bullet} : \mathcal{P}_{\circ} \rightarrow \mathcal{P}_{\bullet}$, and $X_{\circ\bullet}$ is an open subset of $BS(p_{\circ\bullet} : \mathcal{P}_{\circ} \rightarrow \mathcal{P}_{\bullet})$.

Caution: Unlike $BS(\mathcal{P})$, the Bott-Samelson variety $BS(\mathcal{P} \rightarrow \mathcal{Q})$ may be singular. For example, if $\mathcal{P} = \{(x, y) : x, y \in \{0, 1\}\}$, $\mathcal{Q} = \{(x, y) : x, y - 1 \in \{0, 1\}\}$, $p(x, y) = (x, y + 1)$, and $\dim(x, y) = x + y$, then $BS(p)$ (with $n = 3$) is the triangle variety (parametrizing points p_1, p_2, p_3 and lines $\ell_{12}, \ell_{23}, \ell_{31}$ in \mathbb{P}^2 with $p_i, p_j \in \ell_{ij}$) and hence singular. Also, $X_{\circ\bullet}$ need not be dense in $BS(\mathcal{P}_{\circ} \rightarrow \mathcal{P}_{\bullet})$; see Section 3.12 (b).

5.6. Relating $X_{\bullet} \cup X_{\bullet, \text{next}}$ to the simpler variety $BS(\mathcal{P}_{\square})$ via $X_{\bullet, \square}$. Let \mathcal{P}_{\square} be the poset of Figure 18. Then $BS(\mathcal{P}_{\square})$ parametrizes hyperplanes V_y and $V_{y'}$, and a codimension 2 subspace $V_x \subset V_y, V_{y'}$. (Of course $V_z = K^n$.) The variety $BS(\mathcal{P}_{\square})$ has one divisorial stratum D_{\square} , corresponding to $V_y = V_{y'}$. This variety will play a central role in the proof.

It will be useful to describe $X_{\bullet} \cup X_{\bullet, \text{next}}$ in terms of $BS(\mathcal{P}_{\square})$ and D_{\square} . We do this by way of a variety $X_{\bullet, \square}$ which is a certain open subset of $BS(p_{\bullet, \square} : \mathcal{P}_{\bullet} \rightarrow \mathcal{P}_{\square})$ (defined in Sect. 5.7) whose image in $BS(\mathcal{P}_{\bullet})$ is $X_{\bullet} \cup X_{\bullet, \text{next}}$, where $p_{\bullet, \square}$ is the morphism of posets depicted in Figure 19.

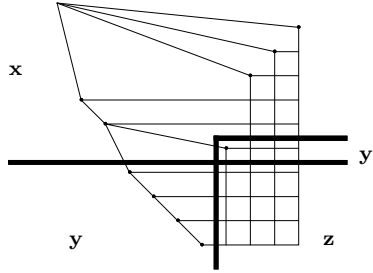


FIGURE 19. A pictorial depiction of $p_{\bullet, \square} : \mathcal{P}_{\bullet} \rightarrow \mathcal{P}_{\square}$; elements of $p_{\bullet, \square}^{-1}(x)$, $p_{\bullet, \square}^{-1}(y)$, $p_{\bullet, \square}^{-1}(y')$, $p_{\bullet, \square}^{-1}(z)$ lie in regions labeled x, y, y', z respectively.

5.7. First description of $X_{\bullet, \square}$. Suppose the descending checker is at (r, c) . Let

$$(3) \quad S_{c-1} \subset S_c \subset \cdots \subset S_n$$

be the subspaces corresponding to elements of \mathcal{P}_{\bullet} in the bottom row of the table (part of the flag F). (Subscripts denote dimension.) Let

$$(4) \quad T_0 \subset T_1 \subset \cdots \subset T_n$$

be the subspaces corresponding to the northeast border of \mathcal{P}_{\bullet} (part of the flag M). Define $X_{\bullet, \square}$ to be the locally closed subvariety of $(X_{\bullet} \cup X_{\bullet, \text{next}}) \times BS(\mathcal{P}_{\square})$ such that

$$(5) \quad V_x \cap T_{r+1} = T_{r-1}, \quad V_{y'} \cap T_{r+1} = T_r, \quad V_y \cap S_c = S_{c-1}.$$

Then the vector spaces corresponding to elements of \mathcal{P}_\bullet are determined by $V_x, V_y, V_{y'}$, and

$$(6) \quad S_c \subset S_{c+1} \subset \cdots \subset S_n, \quad T_0 \subset T_1 \subset \cdots \subset T_{r-2} \subset T_{r+1} \subset \cdots \subset T_{n-1} \subset T_n$$

as shown in Figure 20. (This is because each element of \mathcal{P}_\bullet and $\mathcal{P}_{\bullet, \text{next}}$ is of the form $\text{inf}(\mathbf{b}, \mathbf{b}')$, for some \mathbf{b}' on the northeast border, and \mathbf{b} in the bottom row of the table; and $V_{\text{inf}(\mathbf{b}, \mathbf{b}')} = V_{\mathbf{b}} \cap V_{\mathbf{b}'}$ for any point of X_\bullet and $X_{\bullet, \text{next}}$. Hence $V_{\text{inf}(\mathbf{b}, \mathbf{b}'})$ is determined by (3) and (4), and thus (6) and $V_x, V_y, V_{y'}$.)

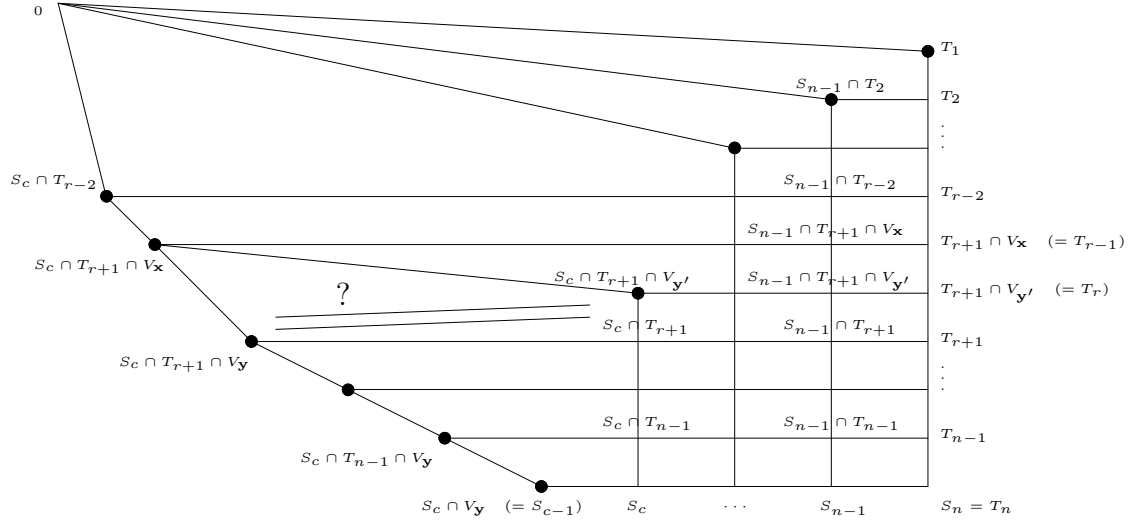


FIGURE 20. Pictorial description of the morphism $X_{\bullet, \square} \rightarrow X_\bullet \cup X_{\bullet, \text{next}}$ (in the guise of the morphism $X_{\bullet, \square} \rightarrow BS(\mathcal{P}_\bullet)$)

5.8. Second description of $X_{\bullet, \square}$. Equivalently, $X_{\bullet, \square}$ parametrizes $V_x, V_y, V_{y'}$, and the partial flags S and T of (6) (not (3) and (4)), such that

- the partial flags S and T are transverse,
- $T_{r-2} \subset T_{r+1} \cap V_x$,
- $V_x \subset V_y, V_{y'}$, and
- V_x is transverse to $S_c \cap T_{r+1}$. (As $r + c \geq n + 1$, $\dim S_c \cap T_{r+1} \geq 2$, so V_y and $V_{y'}$ are also transverse to $S_c \cap T_{r+1}$.)

If these conditions hold, we say that $V_x, V_y, V_{y'}, S, T$, are in $X_{\bullet, \square}$ -position.

The projection $f_{\bullet, \text{next}} : X_{\bullet, \square} \rightarrow X_\bullet \cup X_{\bullet, \text{next}}$ is smooth and surjective: given an element of $X_\bullet \cup X_{\bullet, \text{next}}$, where S and T are the partial flags of (3) and (4), the fiber corresponds to a choice of $(V_x, V_y, V_{y'})$ satisfying (5). More precisely, (i) let $V_y = T_{r-1} + S_{c-1}$, (ii) then choose V_x in V_y such that $V_x \cap T_{r+1} = T_{r-1}$ (or equivalently such that $V_x \supset T_{r-1}$), (iii) then let $V_{y'} = V_x + T_r$.

Similarly, the morphism $f_{\square} : X_{\bullet\square} \rightarrow BS(\mathcal{P}_{\square})$ is smooth and surjective; by the definition of $X_{\bullet\square}$ -position, f_{\square} expresses $X_{\bullet\square}$ as an open subset of a tower of projective bundles over $BS(\mathcal{P}_{\square})$.

5.9. Note that $f_{\bullet\bullet\text{next}}^{-1} X_{\bullet\text{next}} = f_{\square}^{-1} D_{\square}$ (see Figure 20 — $V_y = V_{y'}$ iff $S_c \cap T_{r+1} \cap V_y = S_c \cap T_{r+1} \cap V_{y'}$). This will allow us to translate questions about codimension one degenerations in the specialization order (involving $X_{\bullet\text{next}} \subset X_{\bullet} \cup X_{\bullet\text{next}}$) to simpler facts about codimension one degenerations relating to $D_{\square} \subset BS(\mathcal{P}_{\square})$. The notation $f_{\bullet\bullet\text{next}}$ and f_{\square} will not be used hereafter.

6. PROOF OF THE GEOMETRIC LITTLEWOOD-RICHARDSON RULE

We now prove (the final version of) the Geometric Littlewood-Richardson rule, Theorem 3.10.

6.1. Strategy of proof. The strategy is as follows. Instead of considering the “divisor at ∞ ” of the closure of $X_{\bullet\bullet}$ in $G(k, n) \times (X_{\bullet} \cup X_{\bullet\text{next}})$, we consider the corresponding divisor on closures of other sets in different spaces, shown in (7). (The varieties $X_{\bullet\bullet\square}$ and $X_{\bullet\square}$ will be defined in Sect. 6.3, and the smoothness and surjectivity of the morphisms of the top row will be established. For convenience, let Z be $\text{Cl}_{BS(\mathcal{P}_{\circ}) \times BS(\mathcal{P}_{\square})} X_{\bullet\bullet\square}$.) There is a “divisor at ∞ ” on each of these varieties that behaves well with respect to pullback by these morphisms; it corresponds to $X_{\bullet\text{next}} \subset X_{\bullet} \cup X_{\bullet\text{next}}$ on the left and $D_{\square} \subset BS(\mathcal{P}_{\square})$ on the right.

(7)

$$\begin{array}{ccc} \text{Cl}_{BS(\mathcal{P}_{\circ}) \times (X_{\bullet} \cup X_{\bullet\text{next}})} X_{\bullet\bullet} & \xleftarrow{\text{sm. surj.}} & \text{Cl}_{BS(\mathcal{P}_{\circ}) \times (X_{\bullet} \cup X_{\bullet\text{next}})} X_{\bullet\bullet\square} & \xrightarrow{\text{sm. surj.}} & Z := \text{Cl}_{BS(\mathcal{P}_{\circ}) \times BS(\mathcal{P}_{\square})} X_{\bullet\bullet\square} \\ \downarrow \text{proper birat'l} & & & & \downarrow \text{closed imm.} \\ \text{Cl}_{G(k, n) \times (X_{\bullet} \cup X_{\bullet\text{next}})} X_{\bullet\bullet} & & & & BS(\mathcal{P}_{\circ} \rightarrow \mathcal{P}_{\square}) \end{array}$$

We first identify the components of $\text{Cl}_{BS(\mathcal{P}_{\circ}) \times (X_{\bullet} \cup X_{\bullet\text{next}})} X_{\bullet\bullet}$ as follows. The components of “the divisor at ∞ ” of $BS(\mathcal{P}_{\circ} \rightarrow \mathcal{P}_{\square})$ of dimension at least $\dim X_{\bullet\square} - 1$ are identified by Theorem 6.7. They are denoted D_S^Z , where S is a certain set of “good quadrilaterals” in the poset \mathcal{P}_{\circ} . This gives a list containing the components of the “divisor at ∞ ” of $Z = \text{Cl}_{BS(\mathcal{P}_{\circ}) \times BS(\mathcal{P}_{\square})} X_{\bullet\bullet\square}$. Via the smooth surjective morphisms of the top row of (7), this immediately gives a list containing the components, denoted D_S , of the “divisor at ∞ ” of $\text{Cl}_{BS(\mathcal{P}_{\circ}) \times (X_{\bullet} \cup X_{\bullet\text{next}})} X_{\bullet\bullet}$.

We say D_S is *geometrically irrelevant* if its image in $G(k, n) \times X_{\bullet\text{next}}$ is of smaller dimension (and *geometrically relevant* otherwise). In Section 6.11, it is shown that all but one or two D_S (corresponding to those described in the Geometric Littlewood-Richardson rule) are geometrically irrelevant. We do this by exhibiting a one-parameter family through a general point of D_S contracted by the morphism to $G(k, n) \times X_{\bullet\text{next}}$.

Next, in Section 6.14, we show that in the one or two geometrically relevant cases D_S appears with multiplicity one in the “divisor at ∞ ”, by showing that D_S^Z appears with multiplicity one in the corresponding divisor on Z .

Finally, these one or two D_S 's map are birational to (and hence map with degree 1 to) $X_{\circ_{\text{stay}}\bullet_{\text{next}}}$ or $X_{\circ_{\text{swap}}\bullet_{\text{next}}}$ (Proposition 6.16).

6.2. Remark. The bijection to puzzles of Section 7 gives a second proof; here is a very quick sketch. Fix a mid-sort configuration $\circ\bullet$. First show that D_X contains both $X_{\circ_{\text{stay}}\bullet_{\text{next}}}$ and/or $X_{\circ_{\text{swap}}\bullet_{\text{next}}}$ (Sect. 6.14). By an easy induction, $\circ\bullet$ arises in the course of a checker game starting with some subsets α and β . Then D_X can have no more components, and these one or two must appear with multiplicity one. Otherwise, choose any γ such that the non-zero effective cycle $D_X - \overline{X}_{\circ_{\text{stay}}\bullet_{\text{next}}}$, $D_X - \overline{X}_{\circ_{\text{swap}}\bullet_{\text{next}}}$, or $D_X - \overline{X}_{\circ_{\text{stay}}\bullet_{\text{next}}} - \overline{X}_{\circ_{\text{swap}}\bullet_{\text{next}}}$ has a non-zero coefficient of the basis element corresponding to γ . Then the number of puzzles with inputs α and β and output γ is strictly less than the Littlewood-Richardson coefficient $c_{\alpha\beta}^\gamma$, giving a contradiction.

One advantage of the proof presented in Section 6 is that in order to generalize the Geometric Littlewood-Richardson rule to other geometric situations (see for example [V2] and Conjecture 4.5), one needs the geometry behind it.

6.3. Reduction to $BS(\mathcal{P}_\square)$. We first reduce much of the argument to statements involving the poset \mathcal{P}_\square (Figure 18) rather than the more complicated \mathcal{P}_\bullet as follows.

The composition of $p_{\circ\bullet} : \mathcal{P}_\circ \rightarrow \mathcal{P}_\bullet$ and $p_{\bullet\square} : \mathcal{P}_\bullet \rightarrow \mathcal{P}_\square$ is the morphism $p_{\circ\square} : \mathcal{P}_\circ \rightarrow \mathcal{P}_\square$ depicted in Figure 21. Let $X_{\circ\square}$ be the open subset of $BS(p_{\circ\square} : \mathcal{P}_\circ \rightarrow \mathcal{P}_\square)$ such that if $\mathbf{b} \in \mathcal{P}_\circ$ and $\mathbf{c} \in \mathcal{P}_\square$, then $V_{\mathbf{b}} \subset V_{\mathbf{c}}$ if and only if $p_{\circ\square}(\mathbf{b}) \prec \mathbf{c}$. (One could call this a “precise Bott-Samelson variety” of the morphism of posets, $PBS(p_{\circ\square})$. Then $X_{\circ\bullet} = PBS(p_{\circ\bullet})|_{X_\bullet}$, $X_{\bullet\square} = PBS(p_{\bullet\square})|_{X_\bullet \cup X_{\bullet_{\text{next}}}}$, and $PBS(p) \subset BS(p)$ is an open immersion for all p . However, to minimize notation, we will not use this terminology.)

Define $X_{\circ\bullet\square}$ as a “triple fibered product” as in Figure 22, i.e. as the indirect limit of the lower part of the figure. Equivalently, $X_{\circ\bullet\square}$ is the open subset of $X_{\circ\bullet} \times_{BS(\mathcal{P}_\circ)} X_{\bullet\square}$ whose image in $BS(\mathcal{P}_\bullet) \times BS(\mathcal{P}_\square)$ is in $X_{\bullet\square}$. Note that $X_{\circ\bullet\square}$ is an open subset of both $X_{\circ\bullet} \times_{X_\bullet \cup X_{\bullet_{\text{next}}}} X_{\bullet\square}$ and $X_{\circ\square} \times_{BS(\mathcal{P}_\square)} X_{\bullet\square}$ (although not in general equal to either), so the projections from $X_{\circ\bullet\square}$ to $X_{\circ\bullet}$ and $X_{\circ\square}$ are both smooth (by base change from $X_{\bullet\square} \rightarrow X_\bullet \cup X_{\bullet_{\text{next}}}$ and $X_{\bullet\square} \rightarrow BS(\mathcal{P}_\square)$). In addition, $X_{\circ\bullet\square} \rightarrow X_{\circ\bullet}$ is surjective; the fiber corresponds to a certain (non-empty, open) choice of $V_x, V_y, V_{y'}$. Similarly, $X_{\circ\bullet\square} \rightarrow X_{\circ\square}$ is surjective. This

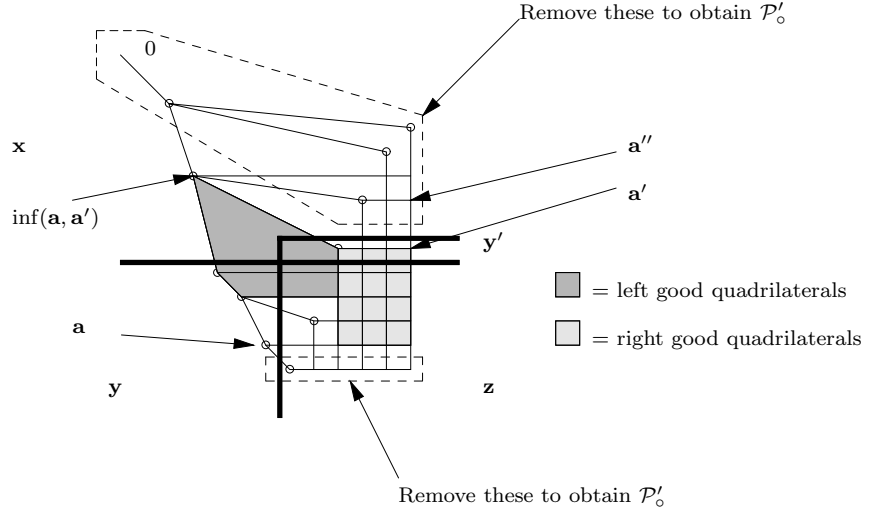


FIGURE 21. $p_{\circ\Box} : \mathcal{P}_{\circ} \rightarrow \mathcal{P}_{\Box}$, $a, a', a'', \mathcal{P}'_{\circ}$

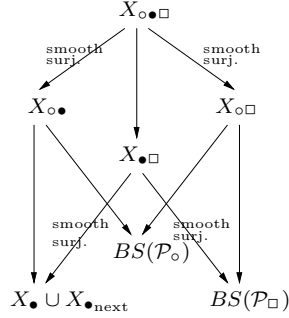


FIGURE 22. The definition of $X_{\circ\Box}$

information is summarized in the top and bottom rows of (8).

$$\begin{array}{ccccc}
 X_{\circ\bullet} & \xleftarrow[\text{surjective}]{\text{smooth}} & X_{\circ\bullet\Box} & \xrightarrow[\text{surjective}]{\text{smooth}} & X_{\circ\Box} \\
 \text{open} \downarrow \text{imm.} & & \text{open} \downarrow \text{imm.} & & \text{open} \downarrow \text{imm.} \\
 (8) \text{ Cl}_{BS(\mathcal{P}_{\circ}) \times (X_{\bullet} \cup X_{\bullet, next})} X_{\circ\bullet} & \xleftarrow[\text{surjective}]{\text{smooth}} & \text{Cl}_{BS(\mathcal{P}_{\circ}) \times X_{\bullet\Box}} X_{\circ\bullet\Box} & \xrightarrow[\text{surjective}]{\text{smooth}} & Z = \text{Cl}_{BS(\mathcal{P}_{\circ}) \times BS(\mathcal{P}_{\Box})} X_{\circ\Box} \\
 \text{proper} \downarrow & & \text{proper} \downarrow & & \text{proper} \downarrow \\
 X_{\bullet} \cup X_{\bullet, next} & \xleftarrow[\text{surjective}]{\text{smooth}} & X_{\bullet\Box} & \xrightarrow[\text{surjective}]{\text{smooth}} & BS(\mathcal{P}_{\Box})
 \end{array}$$

As remarked earlier, $\text{Cl}_{BS(\mathcal{P}_{\circ}) \times BS(\mathcal{P}_{\Box})} X_{\circ\Box}$ is denoted by Z . The morphism

$$\text{Cl}_{BS(\mathcal{P}_{\circ}) \times X_{\bullet\Box}} X_{\circ\bullet\Box} \rightarrow \text{Cl}_{BS(\mathcal{P}_{\circ}) \times (X_{\bullet} \cup X_{\bullet, next})} X_{\circ\bullet}$$

is smooth and surjective for the same reason that $X_{\bullet\bullet\Box} \rightarrow X_{\bullet\bullet}$ and $X_{\bullet\Box} \rightarrow X_{\bullet} \cup X_{\bullet\text{next}}$ were: the fiber corresponds to choosing $V_x, V_y, V_{y'}$, satisfying the requirements of $X_{\bullet\Box}$ -position, except the transversality conditions with the spaces corresponding to elements of \mathcal{P}_{\bullet} , so this morphism is a tower of projective bundles.

6.4. The morphism $\text{Cl}_{BS(\mathcal{P}_{\circ}) \times X_{\bullet\Box}} X_{\bullet\bullet\Box} \rightarrow Z$ is smooth for the same reason that $X_{\bullet\bullet\Box} \rightarrow X_{\bullet\Box}$ and $X_{\bullet\Box} \rightarrow BS(\mathcal{P}_{\circ})$ were. More precisely, this morphism is constructed by choosing the S 's and T 's in (6):

- (i) inductively choosing S_i (starting with $i = n$ and decrementing) so that S_i contains (the subspace corresponding to) the maximum element of \mathcal{P}_{\circ} in column up to i , then
- (ii) inductively choosing T_i (starting with $i = n$ and decrementing) so that T_i contains (the subspace corresponding to) the maximum element of \mathcal{P}_{\circ} in row up to i , then
- (iii) discarding the closed subset not in $X_{\bullet\Box}$ -position, and defining T_{r-1}, T_r, S_{c-1} by (5).

Note that (i) involves only the southwest border of \mathcal{P}_{\circ} (and not the element a shown in Figure 21), and (ii) involves only the northeast border (and not the elements a' and a'' shown in Figure 21).

6.5. Proof of the Geometric Littlewood-Richardson rule in the cases where $p_{\circ\Box}^{-1}(\mathbf{y})$ or $p_{\circ\Box}^{-1}(\mathbf{y}')$ is empty. This corresponds to the cases where there are no white checkers in the critical diagonal or the critical row, respectively (five of the nine cases of Table 2).

In the case $p_{\circ\Box}^{-1}(\mathbf{y}') = \{\}$, the family $Z \rightarrow BS(\mathcal{P}_{\circ})$ is pulled back from a family over $BS(\mathcal{P}_{\circ} - \{\mathbf{y}'\})$, the partial flag parametrizing $V_x \subset V_y \subset K^n$. In particular, the pullback of $D_{\Box} = \{V_y = V_{y'}\}$ to Z consists of one component, appearing with multiplicity 1. The corresponding divisor on $\text{Cl}_{BS(\mathcal{P}_{\circ}) \times (X_{\bullet} \cup X_{\bullet\text{next}})} X_{\bullet\bullet}$ also appears with multiplicity 1 by the top row of (7) or the middle row of (8), and it is isomorphic to its image $\overline{X}_{\text{ostay}\bullet\text{next}}$ in $\overline{X}_{\bullet\bullet}$.

The same argument holds for the case $p_{\circ\Box}^{-1}(\mathbf{y}) = \{\}$, with the roles of \mathbf{y} and \mathbf{y}' switched.

6.6. Proof in the remaining cases. For the rest of Section 6, we assume that both $p_{\circ\Box}^{-1}(\mathbf{y})$ (the critical diagonal) and $p_{\circ\Box}^{-1}(\mathbf{y}')$ (the critical row) are non-empty. The white checkers are in mid-sort, by Lemma 2.8. Let a (resp. a', a'') be the maximum of $p_{\circ\Box}^{-1}(\mathbf{y})$ (resp. $p_{\circ\Box}^{-1}(\mathbf{y}')$, $p_{\circ\Box}^{-1}(\mathbf{x})$), so $V_a, V_{a'}, V_{a''}$ are the corresponding subspaces. (See Figure 21.)

In lieu of studying the components of the preimage of D_{\Box} on Z , we find the components of the pullback of D_{\Box} to the (a priori larger) variety $BS(\mathcal{P}_{\circ} \rightarrow \mathcal{P}_{\circ})$, and show that they all have dimension at most $\dim X_{\circ\Box} - 1$.

The pullback of D_{\Box} to $BS(\mathcal{P}_{\circ} \rightarrow \mathcal{P}_{\circ})$ is best described in terms of the stratification of $BS(\mathcal{P}_{\circ})$. Define the *good quadrilaterals* of \mathcal{P}_{\circ} to be those quadrilaterals whose minimal element does not dominate a , and either (a) whose minimal element dominates the white checker $\min(p_{\circ\Box}^{-1}(\mathbf{y}'))$ in the critical row $p_{\circ\Box}^{-1}(\mathbf{y}')$, or (b) with two vertices dominating $\min(p_{\circ\Box}^{-1}(\mathbf{y}'))$, and two vertices in $p_{\circ\Box}^{-1}(\{\mathbf{x}, \mathbf{y}\})$. Call those in case (a) *right good quadrilaterals*

and those in case (b) *left good quadrilaterals*; see Figure 21. Note that the good quadrilaterals appear in columns, and that, if there is a blocker, there is no column to the left of the white checker in the critical row $\min(p_{\circ\Box}^{-1}(\mathbf{y}'))$ (i.e. no left good quadrilaterals).

The following theorem describes the pullback of D_{\Box} to $BS(\mathcal{P}_{\circ} \rightarrow \mathcal{P}_{\Box})$.

6.7. Theorem. — *The components of the pullback of D_{\Box} to $BS(\mathcal{P}_{\circ} \rightarrow \mathcal{P}_{\Box})$ of dimension at least $\dim X_{\circ\Box} - 1$ correspond to sets of good quadrilaterals, with at most one quadrilateral in each column, as follows. If S is such a set of good quadrilaterals, the corresponding component is the closure of the pullback to $BS(\mathcal{P}_{\circ} \rightarrow \mathcal{P}_{\Box})$ of the open stratum on $BS(\mathcal{P}_{\circ})$ corresponding to S . Its dimension is exactly $\dim X_{\circ\Box} - 1$.*

Let D_S^Z be the component corresponding to S . Let D_S be the corresponding subvariety of $BS(\mathcal{P}_{\circ}) \times X_{\bullet_{\text{next}}}$ (obtained via the top row of (7) or the middle row of (8)).

Proof. We note first that $X_{\circ\Box}$ can be constructed by starting with the dense open stratum of $BS(\mathcal{P}_{\circ})$, then choosing $V_{\mathbf{y}}$ containing $V_{\mathbf{a}}$ and $V_{\mathbf{a}''}$ (giving a dimensional contribution of $n - (\dim \mathbf{a} + \dim \mathbf{a}'' - \dim \inf(\mathbf{a}, \mathbf{a}'))$, as $V_{\mathbf{a}} \cap V_{\mathbf{a}''} = V_{\inf(\mathbf{a}, \mathbf{a}')}$ for an element of the dense open stratum), then choosing $V_{\mathbf{y}'}$ containing $V_{\mathbf{a}'}$ (giving a dimensional contribution of $n - \dim \mathbf{a}'$). Then $V_{\mathbf{x}} = V_{\mathbf{y}} \cap V_{\mathbf{y}'}$ is determined. Hence

$$(9) \quad \dim X_{\circ\Box} = 2n - \dim \mathbf{a} - \dim \mathbf{a}' - \dim \mathbf{a}'' + \dim \inf(\mathbf{a}, \mathbf{a}').$$

Next, consider an irreducible component of the pullback of D_{\Box} to $BS(\mathcal{P}_{\circ} \rightarrow \mathcal{P}_{\Box})$ of dimension at least $\dim X_{\circ\Box} - 1$. We will show that its dimension is precisely this, and that the component is of the form described in Theorem 6.7.

Let $\ell = \dim(V_{\mathbf{a}} \cap V_{\mathbf{a}'}) - \dim \inf(\mathbf{a}, \mathbf{a}')$ for a general point of this component. (Note that $\ell \geq 0$, as $V_{\mathbf{a}} \cap V_{\mathbf{a}'}$ contains $V_{\inf(\mathbf{a}, \mathbf{a}')}$.) Let $Q_{\ell} \subset BS(\mathcal{P}_{\circ})$ be the locus where $\dim(V \cap V') = \ell + \dim \inf(\mathbf{a}, \mathbf{a}')$. Then a dense open subset U of the component with a morphism to Q_{ℓ} , and U is an open set of the fibration over Q_{ℓ} parametrizing choices of $V_{\mathbf{y}} = V_{\mathbf{y}'}$ containing $V_{\mathbf{a}}$ and $V_{\mathbf{a}'}$ (giving a dimensional contribution of $n - (\dim V_{\mathbf{a}} + \dim V_{\mathbf{a}'} - \dim(V_{\mathbf{a}} \cap V_{\mathbf{a}'}))$), and $V_{\mathbf{x}}$ contained in $V_{\mathbf{y}} = V_{\mathbf{y}'}$ containing $V_{\mathbf{a}''}$ (giving a dimensional contribution of $n - 1 - \dim V_{\mathbf{a}''}$ once $V_{\mathbf{y}} = V_{\mathbf{y}'}$ is chosen). Thus by Proposition 6.8 below,

$$\begin{aligned} \dim U &\leq \dim Q_{\ell} + (n - \dim \mathbf{a} - \dim \mathbf{a}' + (\ell + \dim \inf(\mathbf{a}, \mathbf{a}'))) + (n - 1 - \dim \mathbf{a}'') \\ &= (\dim Q_{\ell} + \ell) + 2n - \dim \mathbf{a} - \dim \mathbf{a}' - \dim \mathbf{a}'' + \dim \inf(\mathbf{a}, \mathbf{a}') - 1 \\ &\leq \dim X_{\circ\Box} - 1 \quad (\text{by (9)}), \end{aligned}$$

and if equality holds, then the the component is of the form desired (also by Proposition 6.8). \square

6.8. Proposition. — *The irreducible components of Q_{ℓ} have codimension at least ℓ in $BS(\mathcal{P}_{\circ})$, and those components of codimension exactly ℓ are strata of the form described in Theorem 6.7.*

Proof. Suppose \mathcal{P}'_{\circ} is defined by removing from \mathcal{P}_{\circ} all rows below \mathbf{a} , and all elements of $p_{\circ\Box}^{-1}(\mathbf{x})$ except $\inf(\mathbf{a}, \mathbf{a}')$ (see Figure 21). As in the proof of Lemma 5.2, the natural morphism $BS(\mathcal{P}_{\circ}) \rightarrow BS(\mathcal{P}'_{\circ})$ is a tower of projective bundles, and the components of Q_{ℓ} on

$BS(\mathcal{P}_\circ)$ are precisely the pullback of components of the analogous Q_ℓ on $BS(\mathcal{P}'_\circ)$. Hence the Proposition follows from the analogous result for $BS(\mathcal{P}'_\circ)$, Proposition 6.9. \square

More precisely, it suffices to prove the result for \mathcal{P}'_\circ of the following form. Fix $r_1 < \dots < r_y$ and $c_1 < \dots < c_x$ where $x, y > 1$, and $r_1 < R_1 < \dots < R_z < r_y$ and $c_2 > C_1 > \dots > C_z > c_1$ ((R_i, C_i) will be location of white checkers not contained in the grid $\{(r_i, c_j)\}$, for example a blocker). Then \mathcal{P}'_\circ is the poset generated by the set $\{(r_1, c_i)\}_{1 \leq i \leq x} \cup \{(r_i, c_1)\}_{1 \leq i \leq y} \cup \{(R_i, C_i)\}_{1 \leq i \leq z}$ (see Sect. 5.4, and Figure 23 for an example). Note that the critical row corresponds to $\{(r_1, c_2), \dots, (r_1, c_x)\}$, the critical diagonal corresponds to $\{(r_2, c_1), \dots, (r_y, c_1)\}$, $\mathbf{a} = (r_y, c_1)$, $\mathbf{a}' = (r_1, c_x)$, and $\inf(\mathbf{a}, \mathbf{a}') = (r_1, c_1)$.

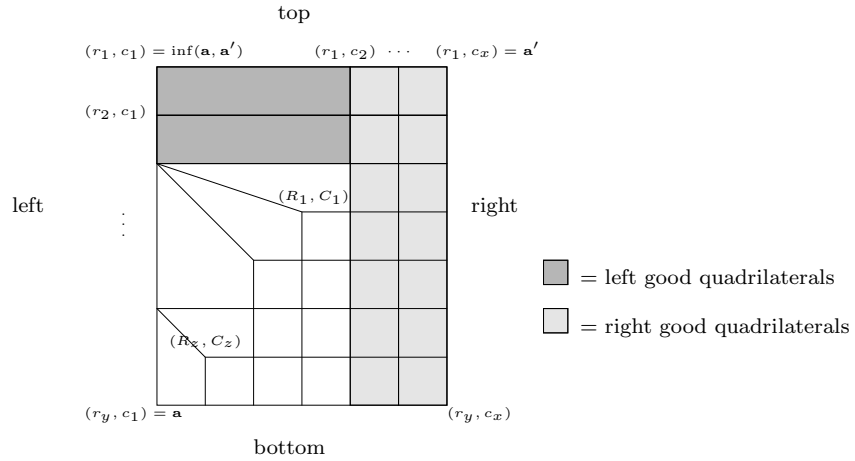


FIGURE 23. An example of \mathcal{P}'_\circ

6.9. Proposition. — *The irreducible components of Q_ℓ on $BS(\mathcal{P}'_\circ)$ (described in the previous paragraph) have codimension at least ℓ in $BS(\mathcal{P}'_\circ)$, and those components of codimension exactly ℓ are strata of the form described in Theorem 6.7 (corresponding to sets of good quadrilaterals, at most one per column).*

Proof. For convenience, we assume $\dim \inf(\mathbf{a}, \mathbf{a}') = 0$. (Geometrically, this corresponds to considering instead the quotient of all subspaces by $V_{\inf(\mathbf{a}, \mathbf{a}')}$.)

Fix an irreducible component of Q_ℓ of codimension at most ℓ , and choose a general point of this component; this corresponds to some configuration of subspaces $\{V_c \subset K^m : \mathbf{c} \in \mathcal{P}'_\circ\}$. Label each element \mathbf{c} of \mathcal{P}'_\circ with $\dim(V_c \cap V_a)$. Hence the label on any vertex dominating \mathbf{a} is $\dim \mathbf{a}$, and the label on \mathbf{a}' is ℓ . The label on any $\mathbf{c} \in \mathcal{P}'_\circ$ is at most $\dim \mathbf{c}$.

This point lies in some open stratum of $BS(\mathcal{P}'_\circ)$; mark the quadrilaterals corresponding to that stratum with “=”. Then each labeled quadrilateral looks like one of the examples in Figure 24.

We argue by induction on the number of good quadrilaterals. The base case is given in (c) and (d) below, and the inductive step is given in (a) and (b).

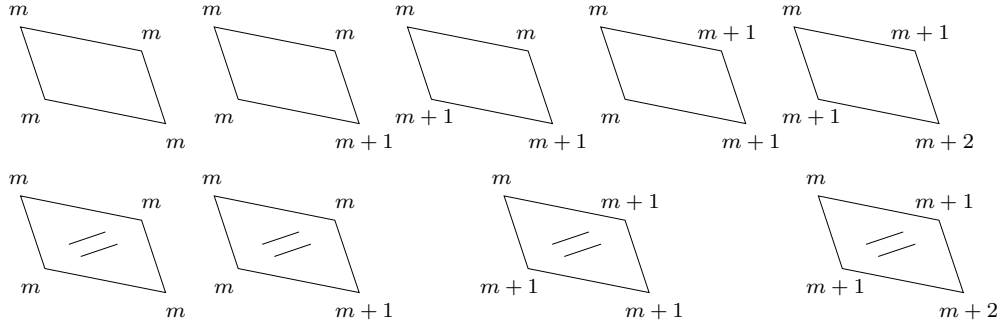


FIGURE 24. Possible quadrilaterals in proof of Proposition 6.9 (where c is labeled with $\dim(V_c \cap V_a)$)

(a) First, if $x > 2$, consider the right-most column of good quadrilaterals (see Figure 25). The two vertices in the bottom row are labeled $\dim a$, and the vertex in the upper right is labeled ℓ . The vertex in the upper left of the column is labeled either $\ell - 1$ or ℓ . If it is labeled ℓ , then the resulting poset with the right-most column of vertices removed also satisfies the hypothesis of the Proposition, and hence by the inductive hypothesis there must be at least ℓ equal signs further to the left, of the desired form (all good quadrilaterals, at most one per column). Hence the Proposition holds in this case.

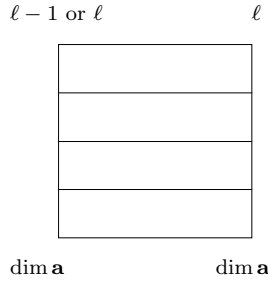


FIGURE 25. The right-most column of quadrilaterals (in case (a) of the proof of Proposition 6.9)

If otherwise the vertex in the upper left corner of the right-most column of quadrilaterals is labeled $\ell - 1$, then by the inductive hypothesis there must be at least $\ell - 1$ equal signs further to the left, of the desired form. Furthermore, by inspection of Figure 24, there must be another equal sign in the right-most column as well, and again the Proposition holds. See Figure 26 for an example.

(b) Next suppose $x = 2$ (so there are no right good quadrilaterals), and there is at least one left good quadrilateral (hence there is no blocker). Let $w = (r_1, c_2)$ (the rightmost element of the top row; this corresponds to the white checker in the critical row of \circ). The label on w must be 0 or 1, as $\dim w = 1$. If w has label 0, then the Proposition follows immediately. If w has label 1, then the top left quadrilateral must be of one of the forms shown in Figure 27. In each case, we can remove the top two vertices of the good

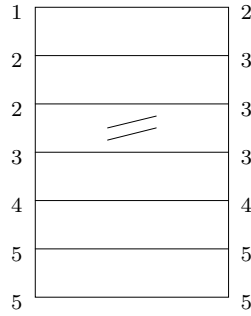


FIGURE 26. Sample labeling of the right-most column of quadrilaterals (in case (a) of the proof of Proposition 6.9)

quadrilateral, and in all but the first case subtract 1 from each of the other vertices (as shown in Figure 27), and reduce to the case with one fewer good quadrilaterals. Hence by the inductive hypothesis, the last case cannot happen (there must be a second “=” in a good quadrilateral further below, yet we are allowed only $\ell = 1$). The other cases may occur, and by our inductive hypothesis the Proposition holds.

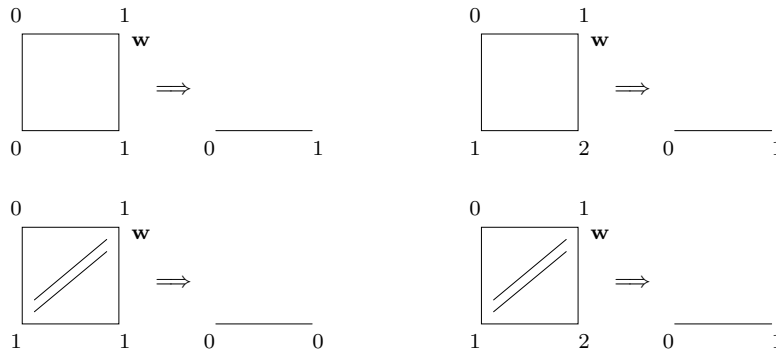


FIGURE 27. The top (left) good quadrilateral (in case (b) of the proof of Proposition 6.9)

(c) Next, if there are no good quadrilaterals, and no blockers, then the labeled poset is the one shown in Figure 28, and the result is immediate.



FIGURE 28. The trivial case (i)(c) of the proof of Proposition 6.9

(d) Finally, suppose there are no good quadrilaterals (implying $x = 2$), and there is a blocker. As in (b), $\ell = 0$ or 1. If $\ell = 0$, the Proposition is immediate.

Assume now that $\ell = 1$; we will obtain a contradiction. Re-label the poset by labeling element c with the dimension of the intersection of its corresponding vector space with $V_{\mathbf{a}'}$ (rather than $V_{\mathbf{a}}$). Hence all labels are 0 or 1, and the elements on the right side and the bottom of the graph are labeled 1. Any quadrilateral with minimal element labeled 0 and other three elements labeled 1 must be marked with an “=” (see Figure 29). By hypothesis, as the component of Q_1 has codimension at most 1 in $BS(\mathcal{P}'_o)$, there can be at most one such quadrilateral. As the subset of elements labeled 0 has a maximum, which doesn't lie on the right side or the bottom of the graph, there is at least one such quadrilateral, so there is exactly one. The component of Q_1 lies in the (irreducible) divisorial stratum corresponding to this quadrilateral, so these two loci are equal. Thus a general point of this divisorial stratum lies in Q_1 .

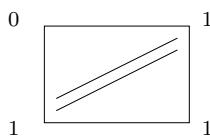


FIGURE 29.

We construct the divisorial stratum as a tower of \mathbb{P}^1 -bundles over the partial flag variety parametrizing the subspaces corresponding to the vertices on the northeast border (as in the proof of Lemma 5.2, where the southwest border was used). There can be no quadrilateral labeled as in Figure 30 (with no “=”): V_e is a general subspace (of dim e) containing V_c and contained in V_f ; as $\dim V_d \cap V_{\mathbf{a}'} = 0$, we have $\dim V_e \cap V_{\mathbf{a}'} = 0$ as well, so the label on the lower left vertex must be 0, not 1.

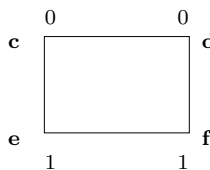


FIGURE 30.

Now consider the part of the graph above row r_2 , as in Figure 31. As there are no quadrilaterals marked as in Figure 30, all unlabeled vertices in Figure 31 must have label 1 (work inductively bottom to top, and left to right in each row), contradicting the fact that there is precisely one quadrilateral marked as in Figure 29. \square

6.10. Remark. The irreducible components of Q_ℓ correspond to sets of good quadrilaterals, at most one per column, such that *each is in a higher row than any to its left*. This describes the components of the pullback of D_\square in Theorem 6.7 completely. To prove this, one must slightly refine case (a) of the proof of Proposition 6.9. However, this fact will not be needed.

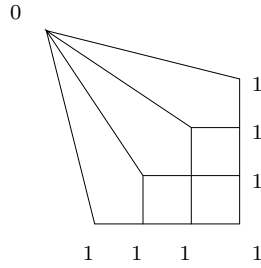


FIGURE 31.

6.11. Geometric irrelevance of all but one or two divisors. We next show that all but one or two of the $D_S \subset BS(\mathcal{P}_\circ) \times X_{\bullet, \text{next}}$ (defined immediately after the statement of Theorem 6.7) are geometrically irrelevant. Note that $D_\{\}$ corresponds to the entry “stay” in Table 2, and $D_{\{\text{top left good quad.}\}}$ corresponds to “swap”.

Proposition 6.12 shows that all other components are geometrically irrelevant, and Proposition 6.13 shows that $D_\{\}$ is geometrically irrelevant as well when required to be by Table 2.

The following example may motivate the argument. Suppose $\circ\bullet$ is the configuration of black and white checkers shown in Figure 32, corresponding to planes in \mathbb{P}^3 . Then a general point of $X_{\circ\bullet}$ is depicted in Figure 33. The four points parametrized by black checkers are denoted b_1, b_2, b_3, b_4 , and the three points parametrized by the white checkers are denoted p_1, p_2, p_3 . The other subspaces parametrized by $BS(\mathcal{P}_\circ)$ are two lines l_{12} and l_{23} (containing $\{p_1, p_2\}$ and $\{p_2, p_3\}$ respectively), and a plane f_{123} . For a fixed point of $X_{\bullet\bullet}$, this locus clearly has dimension 2, (generically) one for the choice of p_2 on the line b_2b_3 and one for the choice of p_3 on the line b_3b_4 .

In the degeneration corresponding to $X_{\bullet, \text{next}}$, b_2 tends to b_1 (and the line of approach ℓ is remembered). Note that there are two good quadrilaterals in \mathcal{P}'_\circ , one “left” and one “right”; denote them L and R . There are then three possible degenerations of Figure 33 (i.e. three components of D'_X), depicted in Figure 34.

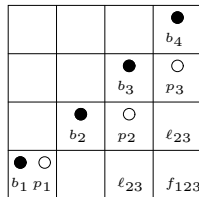


FIGURE 32.

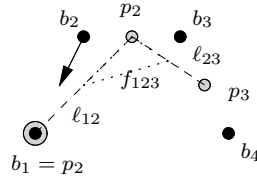


FIGURE 33. A general point of X_{\bullet} . (where $\circ\bullet$ is given in Figure 32)

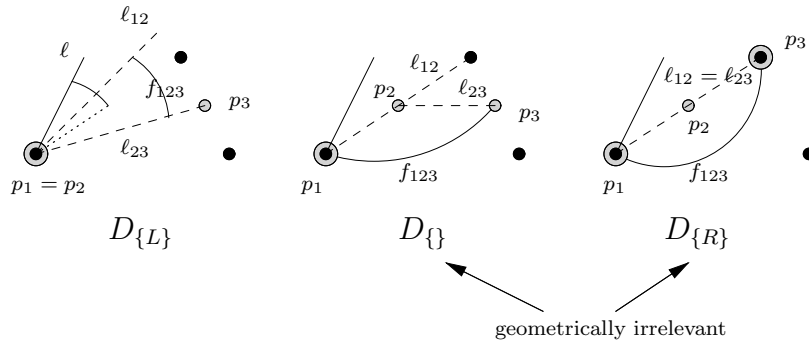


FIGURE 34. Degenerations of Figure 33 (planes are denoted by arcs; a plane contains a line if the arc meets the line)

The first corresponds to the subset $S = \{L\}$, and is geometrically *relevant*. For a fixed point of $X_{\bullet_{\text{next}}}$, this locus visibly has dimension 2, one for the choice of l_{12} through $p_1 = p_2 = b_1 = b_2$ in the plane spanned by ℓ and b_3 , and one for the choice of p_3 on the line b_3b_4 .

The second corresponds to the subset $S = \{\}$, and is geometrically *irrelevant*. For a fixed point of $X_{\bullet_{\text{next}}}$, this locus visibly has dimension 2, one for the choice of p_2 on the line b_1b_3 , and one for the choice of p_3 on the line b_3b_4 . However, the image in $G(3, 4) = \mathbb{G}(2, 3)$ has dimension 1, as the plane f_{123} depends only on the choice of p_3 . This observation is a special case of Proposition 6.13.

The third corresponds to the subset $\{R\}$, and is also geometrically *irrelevant*. For a fixed point of $X_{\bullet_{\text{next}}}$, this locus visibly has dimension 2, one for the choice of p_2 on the line b_1b_3 , and one for the choice of the plane f_{123} containing the line b_1b_3 . Again, the image in $G(3, 4)$ has dimension 1. This observation is a special case of Proposition 6.12.

Note that there is no component corresponding to $S = \{L, R\}$, as the locus $Q_{\ell=2}$ on $BS(\mathcal{P}_{\circ})$ is empty (as $\dim \mathbf{a} = \dim \mathbf{a}' = 1$, so $\ell := \dim V_{\mathbf{a}} \cap V_{\mathbf{a}'} - \dim V_{\inf(\mathbf{a}, \mathbf{a}')} \leq 1 - 0 = 1$).

6.12. Proposition. — *If $S \neq \{\}$, {top left good quad.}, then D_S is geometrically irrelevant.*

Proof. Note that the projection

$$\mathrm{Cl}_{BS(\mathcal{P}_\circ) \times (X_\bullet \cup X_{\bullet \text{next}})} X_{\circ\bullet} \rightarrow \mathrm{Cl}_{G(k,n) \times (X_\bullet \cup X_{\bullet \text{next}})} X_{\circ\bullet}$$

involves forgetting all elements of \mathcal{P}_\circ but the maximum, and that its construction (given in Sect. 6.4) depends only on the vector spaces on the northeast and southeast borders of \mathcal{P}_\circ . Fix a general point of D_S^Z (corresponding to a configuration of subspaces $\{V_c \subset K^n : c \in \mathcal{P}_\circ\}$). It will suffice to produce a one-parameter family through this point that preserves the spaces in the northeast and southwest borders. All possibilities for S fall into at least one of the following three cases.

Case 1: S contains a left good quadrilateral that is not the top left good quadrilateral. Name the elements of \mathcal{P}_\circ as in Figure 35 (showing the quadrilateral in question). Then a one-parameter family corresponds to fixing all V_m ($m \in \mathcal{P}_\circ$) except V_d , and letting V_d move freely in $\mathbb{P}(V_b/V_e) \cong \mathbb{P}^1$.

(Note that this would fail if the left good quadrilateral were at the top. In this case, $p_{\circ\Box}(d) = \mathbf{x}$, but the V_d corresponding to a general element of $\mathbb{P}(V_b/V_e)$ would lie in $V_y = V_{y'}$, and not necessarily in V_x .)

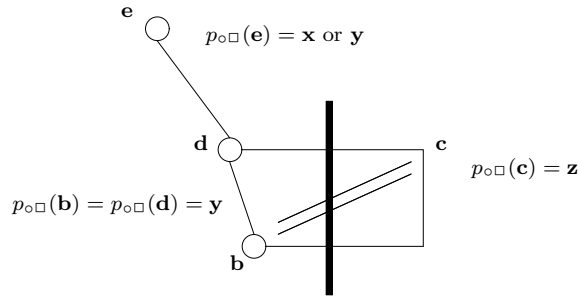


FIGURE 35. Case 1 of Proposition 6.12

Case 2: S contains a right good quadrilateral q , and no quadrilaterals in the column directly to the left of q , and at least as high as q . Name the elements of \mathcal{P}_\circ as in Figure 36. The desired one-parameter family corresponds to fixing all the vector spaces V_m ($m \in \mathcal{P}_\circ$) except for $V_d, V_{g_1}, \dots, V_{g_m}$, and choosing V_d from an open set of $\mathbb{P}(V_b/V_e) \cong \mathbb{P}^1$, such that $V_{g_i} := V_d \cap V_{h_i}$ has dimension $\dim g_i$ ($1 \leq i \leq m$). Note that V_{f_i} is automatically contained in V_{g_i} as $V_{g_i} = V_d \cap V_{h_i}$ contains $V_e \cap V_{h_i} = V_{f_i}$ by construction.

Case 3: S contains a right good quadrilateral q , and another good quadrilateral in the column directly to the left of q , at least as high as q . Name the elements of \mathcal{P}_\circ as in Figure 37. Then the argument from the Case 2 applies verbatim. \square

6.13. Proposition. — If $S = \{\}$ and (i) the white checker in the critical row is in the descending checker's square, or (ii) the white checker in the critical diagonal is in the rising checker's square, then D_S is geometrically irrelevant.

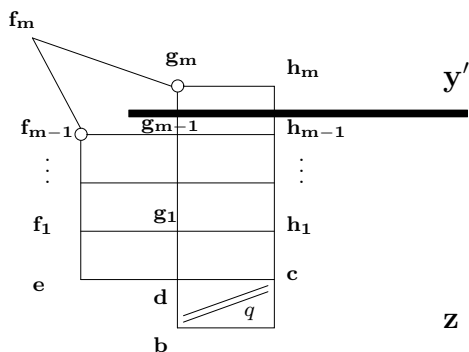


FIGURE 36. Case 2 of Proposition 6.12

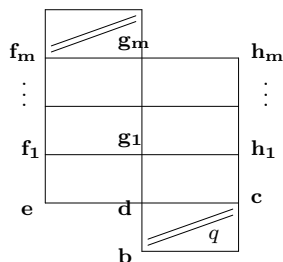


FIGURE 37. Case 3 of Proposition 6.12

Proof. We deal with case (ii); case (i) is essentially identical and hence omitted.

As in the proof of Proposition 6.12, we note that the construction of Section 6.4 depended only on the vector spaces on the northeast and southeast borders of \mathcal{P}_\circ , but *not* the vector space on the northeast border in the critical row. Hence it will suffice to produce a one-parameter family through a general point of D_S^Z that preserves the spaces in the northeast and southwest borders, except the element of the critical row.

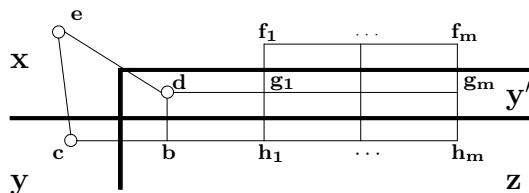


FIGURE 38.

Name the elements of \mathcal{P}_\circ as in Figure 38. As the point of D_S^Z maps to the dense open stratum of $BS(\mathcal{P}_\circ)$, we have $V_{h_i} = V_c + V_{g_i}$; as $V_c \subset V_y = V_{y'}$ and $V_{g_i} \subset V_{y'}$, we have $V_{h_i} \subset$

V_y as well. The desired one-parameter family corresponds to fixing all the vector spaces V_l ($l \in \mathcal{P}_\circ$) except for $V_d, V_{g_1}, \dots, V_{g_m}$, and choosing V_d from an open set of $\mathbb{P}(V_b/V_e) \cong \mathbb{P}^1$, such that $V_{g_i} := V_d + V_{f_i}$ has dimension $\dim g_i$ ($1 \leq i \leq m$). \square

6.14. Multiplicity 1. We have shown that at most one or two of the components of D'_X are geometrically relevant. We now show that these one or two components appear with multiplicity 1 in $\text{Cl}_{BS(\mathcal{P}_\circ) \times (X_\bullet \cup X_{\bullet \text{next}})} X_{\circ\bullet}$. By the top row of (7) or the middle row of (8), it suffices to prove that the analogous divisors on Z appear with multiplicity 1.

6.15. Proposition. —

- (a) The divisor $D_{\{\}}^Z$ is contained in the pullback of D_\square with multiplicity 1.
- (b) The divisor $D_{\{\text{top left good quad.}\}}^Z$ is contained in the pullback of D_\square with multiplicity 1 if there is no blocker (i.e. there is a top left good quadrilateral).

Proof. (a) It suffices to verify the result in the preimage of the dense open stratum of $BS(\mathcal{P}_\circ)$; it then suffices to verify the result for a fixed point of $BS(\mathcal{P}_\circ)$. Here

$$V_{\mathbf{a}} \cap V_{\mathbf{a}'} = V_{\mathbf{a}} \cap V_{\mathbf{a}''} = V_{\inf(\mathbf{a}, \mathbf{a}')}.$$

The Proposition then reduces to a straightforward (hence omitted) local calculation about the locus in $BS(\mathcal{P}_\square)$ such that V_x contains $V_{\mathbf{a}''}$, V_y contains $V_{\mathbf{a}'}$, and $V_{y'}$ contains $V_{\mathbf{a}'}$ (where $V_{\mathbf{a}}, V_{\mathbf{a}'}, V_{\mathbf{a}''}$ are fixed).

(b) It suffices to verify the result in the preimage of the union of the dense open stratum of $BS(\mathcal{P}_\circ)$ and the (divisorial) open stratum of $BS(\mathcal{P}_\circ)$ corresponding to {top left good quad.}. This union admits a \mathbb{P}^1 -fibration to the divisorial stratum of $BS(\mathcal{P}_\circ)$, and it suffices to verify the result for a fixed fiber as follows. Name the elements of \mathcal{P}_\circ as in Figure 38. (Note that $\mathbf{a}' = \mathbf{g}_m$, $\mathbf{a}'' = \mathbf{f}_m$, $\mathbf{e} = \inf(\mathbf{a}, \mathbf{a}')$.) Hold fixed all the spaces of \mathcal{P}_\circ except those in the critical row $\{V_d, V_{g_1}, \dots, V_{g_m}\}$. The space V_d corresponding to the white checker varies in $\mathbb{P}(V_b/V_e)$, and V_{g_i} is defined to be $V_d + V_{f_i}$. The Proposition then reduces to a straightforward (hence omitted) local calculation about the space parametrizing $(V_x, V_y, V_{y'}, V_d)$ such that V_d varies in the pencil, V_x contains the fixed space V_{f_m} , V_y contains the fixed space $V_{\mathbf{a}'}$ and $V_{y'}$ contains $V_{g_m} = V_d + V_{f_m}$. \square

Finally, we show that the map from D_S to $\text{Cl}_{G(k,n) \times (X_\bullet \cup X_{\bullet \text{next}})} X_{\circ\bullet}$ is birational to $\overline{X}_{\circ_{\text{stay}} \bullet \text{next}}$ or $\overline{X}_{\circ_{\text{swap}} \bullet \text{next}}$; this will conclude the proof of the Geometric Littlewood-Richardson rule.

6.16. Proposition. — (a) $D_{\{\}}$ is birational to $\overline{X}_{\circ_{\text{stay}} \bullet \text{next}}$. (b) $D_{\{\text{top left good quad.}\}}$ is birational to $\overline{X}_{\circ_{\text{swap}} \bullet \text{next}}$.

Proof. (a) The open subset of $D_{\{\}}$ contained in the preimage of the dense open stratum of $BS(\mathcal{P}_\circ)$ is isomorphic to $X_{\circ_{\text{stay}} \bullet \text{next}}$. *Sketch of reason:* The subspaces parametrized by the dense open stratum are determined by the subspaces corresponding to the white checkers. (For $\mathbf{c} \in \mathcal{P}_\circ$, $V_{\mathbf{c}} = \text{span}(V_{\mathbf{w}})$, where \mathbf{w} runs over the white checkers dominated by

c.) As in the construction of Section 6.4, choose (i) S_i to contain those V_w where w is a white checker in column at most i , and to contain no V_w where w is a white checker in column greater than i , and (ii) T_i analogously. This gives a subset of the “divisor at ∞ ” of $\text{Cl}_{BS(\mathcal{P}_\circ) \times (X_\bullet \cup X_{\bullet, \text{next}})} X_{\circ\bullet\blacksquare}$ whose image in $\text{Cl}_{BS(\mathcal{P}_\circ) \times (X_\bullet \cup X_{\bullet, \text{next}})} X_{\circ\bullet}$ is $X_{\circ\text{stay}\bullet, \text{next}}$.

(b) The open subset of $D_{\{\text{top left good quad.}\}}$ contained in the preimage of the divisorial open stratum of $BS(\mathcal{P}_\circ)$ corresponding to $\{\text{top left good quad.}\}$ is isomorphic to $X_{\circ\text{swap}\bullet, \text{next}}$. *Sketch of reason:* The subspaces parametrized by the divisorial open stratum are determined by the subspaces corresponding to

- (i) the white checkers of \circ , except the white checkers at the opposite corners of the top left good quadrilateral (call them $w_1 = (r_1, c_1)$, $w_2 = (r_2, c_2)$, with $r_1 > r_2$, $c_1 < c_2$),
- (ii) the vector space $V_{w_1} = V_{w_2}$, and
- (iii) $V_{\text{sup}(w_1, w_2)}$ (corresponding to the lower right corner of the top left good quadrilateral).

We can interpret these subspaces as follows. Identify w_1 and w_2 of \mathcal{P}_\circ to obtain the poset $\mathcal{P}_{\circ\text{swap}}$. The spaces described above correspond to those elements of $\mathcal{P}_{\circ\text{swap}}$ with exactly one edge to a lower-dimensional element (i.e. those w such that there is a unique covering relation $w' \prec w$). They also correspond to the white checkers of $\circ\text{swap}$. As in (a), the image in $\text{Cl}_{BS(\mathcal{P}_\circ) \times (X_\bullet \cup X_{\bullet, \text{next}})} X_{\circ\bullet}$ is (naturally isomorphic to) $X_{\circ\text{swap}\bullet, \text{next}}$. (The white checker of $\circ\text{swap}$ corresponding $V_{w_1} = V_{w_2}$ must lie in the intersection of the spaces where V_{w_1} and V_{w_2} were required to lie, in the definition of $X_{\circ\bullet}$. Hence this checker lies in (r_2, c_1) . The white checker of $\circ\text{swap}\bullet, \text{next}$ corresponding to $V_{\text{sup}(w_1, w_2)}$ is required to lie in (r_1, c_2) , as it was in $X_{\circ\bullet}$.) \square

7. APPENDIX: THE BIJECTION BETWEEN CHECKER GAMES AND PUZZLES (WITH A. KNUTSON)

Fix k and n . We fill in a puzzle with given inputs, one row of triangles at a time, from left to right. Row m consists of those triangles between the m^{th} edges from the top on the sides of the triangle.

The placement of vertical rhombi may cause parts of subsequent rows to be filled; call these *teeth*. The m^{th} row ($1 < m \leq n$) corresponds to the part of the checker game where the black checker in the m^{th} column is descending. The possible choices for filling in puzzle pieces correspond to the possible choices of next moves in the checker game; this will give the bijection.

We now describe an injection from checker games to puzzles; to each checker game we will associate a puzzle. As both count Littlewood-Richardson coefficients, this injection must be a bijection. Alternatively, to show that this is a bijection, one can instead show that there are no puzzles not accounted for here. For example, one can show easily that there are no puzzles if the checker game predicts there shouldn't be (i.e. if the sets are $a_1 < \dots < a_k$ and $b_1 < \dots < b_k$, and if $a_i + b_{k+1-i} \leq n$ for some i), by focusing on a certain

parallelogram-shaped region of the puzzle. More generally, one should be able to show combinatorially that if a partially-filled-in puzzle doesn't correspond to a valid checker game (in progress), then there is no way to complete it.

7.1. Bijection of starting positions. Fill in the top row of the puzzle in the only way possible. (As remarked earlier, the translation to checkers will give an immediate criterion for there to be no puzzles.)

7.2. The translation part-way through the checker game. At each stage, the partially complete puzzle will look like Figure 39. Any of a , b , and c may be zero. In the checker game, a , b , and c correspond to the numbers shown in Figure 40. The rows of the white checkers in the game are given by the edges of Figure 41 — a “1” indicates that there is a white checker in that row. The columns are given by the edges of Figure 42. As the white checkers are mid-sort, it turns out that this specifies their position completely. See Figure 43 for a more explicit description.

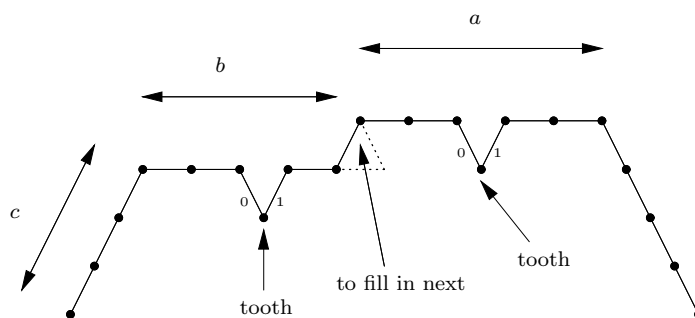


FIGURE 39. The puzzle in the process of being filled

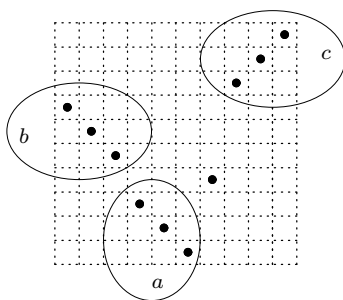


FIGURE 40. The corresponding point in the checker game

We now go through the various cases of how to fill in the next part of the puzzle, and verify that they correspond to the possible next moves of the checker games. Each case is depicted in Figure 44, along with the portion of Table 2 that it corresponds to (in

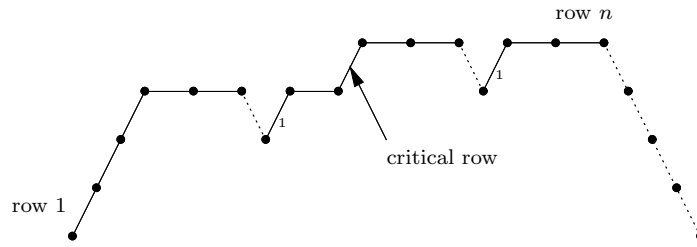


FIGURE 41. The rows of the white checkers

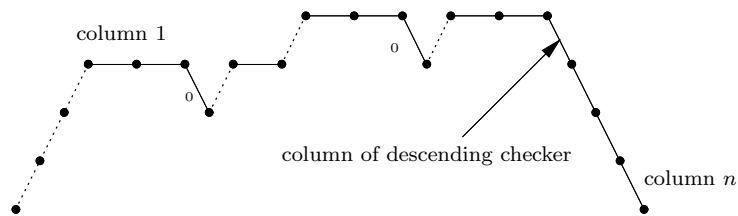


FIGURE 42. The columns of the white checkers

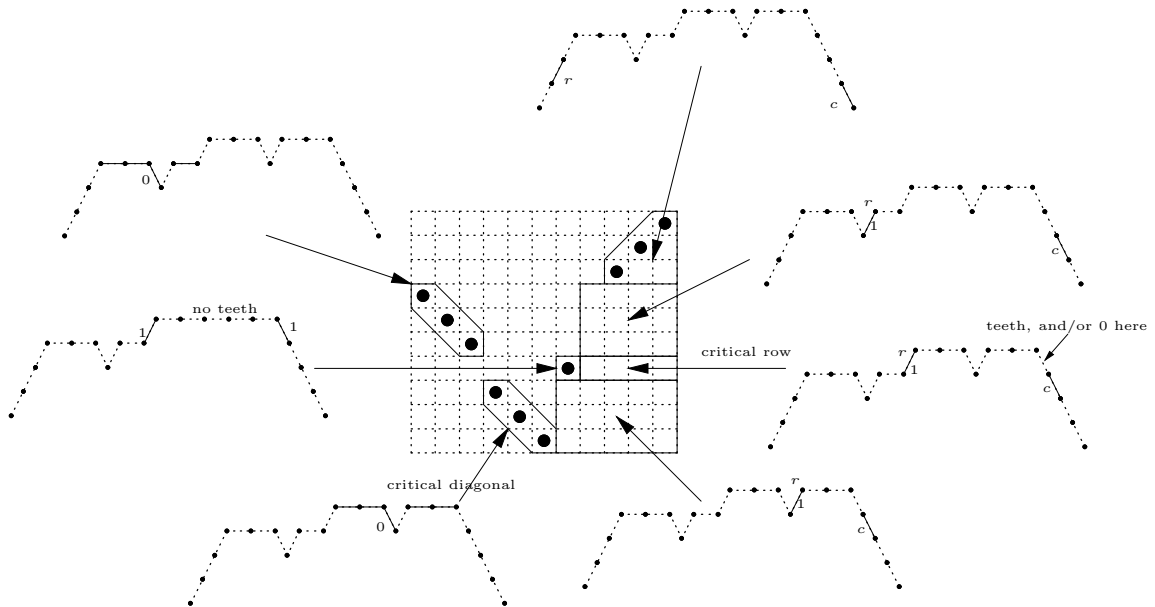


FIGURE 43. How to locate the white checker given the partially completed puzzle (r is the row and c is the column; see Figures 40 and 42 to interpret them as numbers)

checkers). The reader should verify that all possible puzzle piece placements, and all possible checker moves, are accounted for in the bijection.

Case 1. There is no white checker in the critical row, or in the next row. Then make one move in the checker game.

Case 2. There is no white checker in the critical row, and there is a white checker in the next row, not on the rising black checker.

Case 3. There is no white checker in the critical row, and there is a white checker on the rising black checker.

Case 4. There is a white checker in the descending checker's square. In this case, we finish the row of the puzzle, and make a series of checker moves to move the descending checker to the bottom row.

Case 5. There is a white checker in the critical row but not in the descending checker's square, and there are no white checkers in any lower row. We finish the row of the puzzle, and make a series of checker moves to move the descending checker to the bottom row.

Case 6. There is a white checker in the critical row, and there is another white checker in a lower row, but in a higher row than any white checkers on the critical diagonal (e.g. a blocker if there is a white checker on the critical diagonal). We finish the part of the row of the puzzle up to the corresponding tooth, and make a series of checker moves to move the descending checker to the blocker's row.

Case 7. There is a white checker in the critical row but not in the descending checker's square, and there is a white checker in the rising checker's square. Then we place two puzzle pieces and make one checker move, as shown.

Case 8. There is a white checker in the critical row, but not on the descending checker; there is a white checker in the critical diagonal, but not on the rising checker; and there is no blocker. Then there are two cases. If the white checkers "stay", then then we make one checker move, and place two pieces. If the white checkers "swap", then we fill in the part of the puzzle until the "1" in the region marked a in Figure 39, and make a series of checker moves to move the descending checker to the row of the lower white checker in question.

REFERENCES

- [B1] A. S. Buch, *A Littlewood-Richardson rule for the K -theory of Grassmannians*, preprint 2000, math.AG/0004137, Acta Math., to appear.
- [B2] A. S. Buch, personal communication.
- [BKT] A. S. Buch, A. Kresch, and H. Tamvakis, *Gromov-Witten invariants on Grassmannians*, preprint 2003, <http://home.imf.au.dk/abuch/papers/>.
- [EH] D. Eisenbud and J. Harris, *Divisors on general curves and cuspidal rational curves*, Invent. Math. **74** (1983), no. 3, 371–418.
- [F] W. Fulton, *Young Tableau with Applications to Representation Theory and Geometry*, Cambridge U.P., New York, 1997.
- [FP] W. Fulton and P. Pragacz, *Schubert varieties and degeneracy loci*, Lecture Notes in Math., 1689, Springer-Verlag, Berlin, 1998.
- [H] W.V.D. Hodge, *The intersection formulae for a Grassmannian variety*, J. Lon. Math. Soc. **17**, 1942, 48–64.
- [K11] S. Kleiman, *The transversality of a general translate*, Compositio Math. **28** (1974), 287–297.

Case	Puzzle Before	Puzzle After	Checker movement	Part of Table 2
1				
2				
3				
4				
5				
6		(same)		
7				
8		<p>stay:</p> <p>or swap:</p>	 	

FIGURE 44. How to place the next piece in the puzzle?

- [K12] S. Kleiman, *Problem 15: Rigorous foundation of Schubert's enumerative calculus*, Mathematical developments arising from Hilbert problems, Proc. Sympos. Pure Math. **28** (1976), 445–482.
- [KT] A. Knutson and T. Tao, *Puzzles and (equivariant) cohomology of Grassmannians*, preprint 2001, math.AT/0112150, Duke Math. J., to appear.

- [KTW] A. Knutson, T. Tao, and C. Woodward, *The honeycomb model of $GL(n)$ tensor products II: Puzzles give facets of the L - R cone*, preprint 2001, math.CO/0107011, J. Amer. Math. Soc., to appear.
- [KL] V. Kreiman and V. Lakshmibai, *Richardson varieties in the Grassmannian*, preprint 2002, math.AG/0203278.
- [P] M. Pieri, *Sul problema degli spazi secanti*, Rendiconti (Reale Istituto lombardo di scienze e lettere), Vol. **26** (1893), 534–546.
- [R] R. W. Richardson, *Intersections of double cosets in algebraic groups*, Indag. Math., (N.S.), **3** (1992), 69–77.
- [S1] F. Sottile, *Enumerative geometry for the real Grassmannian of lines in projective space*, Duke Math. J., **87** (1997), pp. 59–85.
- [S2] F. Sottile, *Pieri’s formula via explicit rational equivalence*, Can. J. Math, **46** (1997), 1281–1298.
- [S3] F. Sottile, *Some real and unreal enumerative geometry for Flag manifolds*, Michigan Math. J. **48** (2000), 573–592.
- [S4] F. Sottile, personal communication.
- [SVV] F. Sottile, R. Vakil, and J. Verschelde, *Effective solutions to all Schubert problems*, work in progress.
- [St1] R. Stanley, *Combinatorial aspects of the Schubert calculus*, Combinatoire et représentation du groupe symétrique (Actes Table Ronde CNRS, Univ. Louis-Pasteur Strasbourg, Strasbourg, 1976), 217–251. Lecture Notes in Math., Vol. 579, Springer, Berlin, 1977.
- [St2] R. Stanley, *Positivity problems and conjectures in algebraic combinatorics*, Mathematics: Frontiers and perspectives, 295–319, Amer. Math. Soc., Providence, RI, 2000.
- [T] T. Tao, personal communication.
- [V1] R. Vakil, *The enumerative geometry of rational and elliptic curves in projective space*, J. Reine Angew. Math. (Crelle) **529** (2000), 101–153.
- [V2] R. Vakil, *Schubert induction*, preprint 2003.

DEPT. OF MATHEMATICS, STANFORD UNIVERSITY, STANFORD CA 94305–2125

E-mail address: vakil@math.stanford.edu